4.

AUTOMATIC GUIDANCE AND CONTROL OF A TRANSPORT AIRCRAFT DURING A HELICAL LANDING APPROACH

Daniel J. Crawford and Roland L. Bowles

Langley Research Center
Hampton, Va. 23665

3.

NATIONAL AERONAUTICS AND SPACE ADMINISTRATION • WASHINGTON, D. C. • SEPTEMBER 1975

5.

1. Report No.	2. Government Accession No.	3. Recipient's Catalog No.
NASA TN D-7980		

4. Title and Subtitle
AUTOMATIC GUIDANCE AND CONTROL OF A TRANSPORT AIRCRAFT DURING A HELICAL LANDING APPROACH

5. Report Date: September 1975

6. Performing Organization Code:

7. Author(s)
Daniel J. Crawford and Roland L. Bowles

8. Performing Organization Report No.: L-10101

9. Performing Organization Name and Address
NASA Langley Research Center
Hampton, Va. 23665

10. Work Unit No.: 023-11-16-05

11. Contract or Grant No.:

12. Sponsoring Agency Name and Address
National Aeronautics and Space Administration
Washington, D.C. 20546

13. Type of Report and Period Covered: Technical Note

14. Sponsoring Agency Code:

15. Supplementary Notes

16. Abstract

Linear optimal regulator theory is applied to a nonlinear simulation of a transport aircraft performing a helical landing approach. A closed-form expression for the quasi-steady nominal flight path is presented along with the method for determining the corresponding constant nominal control inputs. The Jacobian matrices and the weighting matrices in the cost functional are time varying. A method of solving for the optimal feedback gains is reviewed. The control system is tested on several alternative landing approaches using both 3^{o} and 6^{o} flight path angles. On each landing approach, the aircraft was subjected to large random initial-state errors and to randomly directed crosswinds. The system was also tested for sensitivity to changes in the parameters of the aircraft and of the atmosphere. Performance of the optimal controller on all the 3^{o} approaches was very good. Mean errors in the lateral, vertical, and longitudinal directions for the principal flight path (270^{o} turn) were 0.8 m, -0.1 m, and -9.4 m. The magnitude of the respective ranges of these errors were 1.0 m, 1.9 m, and 26.7 m. The control system proved to be reasonably insensitive to parametric uncertainties. Performance was not as good on the 6^{o} approaches. On the principal flight path, mean errors for the lateral, vertical, and the longitudinal directions were 9.4 m, -0.4 m, and -2.9 m and the magnitude of the respective ranges for these errors were 8.7 m, 3.2 m, and 45.2 m. A modification to the 6^{o} flight path is proposed for the purpose of improving performance.

17. Key Words (Suggested by Author(s))	18. Distribution Statement
Automatic guidance Optimum control Helical landing approach Quasi-steady landing approach Regulator problem Four-dimensional landing approach	Unclassified – Unlimited Subject Category 08

19. Security Classif. (of this report)	20. Security Classif. (of this page)	21. No. of Pages	22. Price*
Unclassified	Unclassified	56	$4.25

*For sale by the National Technical Information Service, Springfield, Virginia 22161

AUTOMATIC GUIDANCE AND CONTROL OF A TRANSPORT AIRCRAFT DURING A HELICAL LANDING APPROACH

Daniel J. Crawford and Roland L. Bowles
Langley Research Center

SUMMARY

Linear optimal regulator theory is applied to a nonlinear simulation of a transport aircraft performing a helical landing approach. A closed-form expression for the quasi-steady nominal flight path is presented along with the method for determining the corresponding constant nominal control inputs. The Jacobian matrices and the weighting matrices in the cost functional are time varying. A method of solving for the optimal feedback gains is reviewed. The control system is tested on several alternative landing approaches using both 3^{o} and 6^{o} flight path angles. On each landing approach, the aircraft was subjected to large random initial-state errors and to randomly directed cross-winds. The system was also tested for sensitivity to changes in the parameters of the aircraft and of the atmosphere. Performance of the optimal controller on all the 3^{o} approaches was very good. Mean errors in the lateral, vertical, and longitudinal directions for the principal flight path (270^{o} turn) were 0.8 m, -0.1 m, and -9.4 m. The magnitude of the respective ranges of these errors were 1.0 m, 1.9 m, and 26.7 m. The control system proved to be reasonably insensitive to parametric uncertainties. Performance was not as good on the 6^{o} approaches. On the principal flight path, mean errors for the lateral, vertical, and the longitudinal directions were 9.4 m, -0.4 m, and -2.9 m and the magnitude of the respective ranges for these errors were 8.7 m, 3.2 m, and 45.2 m. A modification to the 6^{o} flight path is proposed for the purpose of improving performance.

INTRODUCTION

Aircraft traffic in the neighborhood of commercial airports has been the subject of intensive study during the past several years. Noise, collision avoidance, airspace congestion, air pollution, and dangerous wing-tip vortices are all problems which are being studied by engineers today. Presently, in the near-terminal area, aircraft typically follow essentially straight-line paths to a common point, where they are sequenced to follow one another down a 3^{o} flight path on a straight-in approach to the runway. This procedure very often results in low-altitude flying at relatively high power settings over residential or densely populated business districts which is objectionable, at least, from a noise

standpoint if not from the standpoint of safety. Recently, steeper, 6° flight paths and two-segment final approaches (ref. 1) have been proposed to eliminate these problems and are currently being tested. This paper proposes an alternative to these procedures. It consists of descent along a helical path to a low altitude where the straight-in final approach is intercepted and followed. This flight path has the advantage of keeping the aircraft at low power and at relatively high altitude except in the immediate area of the airport. The approach path is helical, the flight-path angle, ground speed, and turning rate are maintained constant during descent, and the control inputs are fixed except to null flight-path errors.

Implementation of the proposed automatic guidance system requires two factors which are not at present universally available. The two factors are an on-board flight control computer and a fairly precise knowledge of the aircraft's position in space. However, with the advent of automatic landing systems, flight computers are becoming much more common on commercial transports and the proposed installation of the microwave landing system (MLS) equipment at airports throughout the country will make the necessary position data available (ref. 1).

The method proposed in this paper uses the theory of optimum control which is treated in references 2 to 6. The theory is applied to a three-degree-of-freedom nonlinear aircraft simulation. In order to pose the problem as a linear regulator, the equations were linearized about a nominal state (helical path) and control trajectory. The resulting near-optimum feedback control gains were then tested in the nonlinear model. This work is an extension of that presented in references 7 and 8. The extension includes increasing the number of states to six and the number of controls to three. The additional states remove the restriction that altitude be monotonically decreasing and the inclusion of thrust (autothrottle) as a control allows treatment of aircraft other than gliders. Reference 7 concerns itself with a HL-10 lifting body reentry vehicle and reference 8 with an unpowered Boeing 707 with no external wind disturbances. Another extension of this work is inclusion of the quasi-steady helical path with its consequent piecewise constant control inputs. This factor greatly reduces the problem of computer storage of the state and control trajectories. The method for computing these quasi-steady paths along with the method for computing appropriate control inputs are presented herein. In addition, a derivation of the equations of motion is given, along with the method of solving for the near-optimum feedback gains. It should be noted that this study, as do those of references 6 and 8, uses angle of attack and bank angle as control inputs. This is a simplification of the dynamic model which does not include control surfaces such as elevators, ailerons, or rudder.

Feedback gains were obtained for several candidate approach paths including both 3° and 6° flight-path angles and turns of 180°, 270°, and 360°. An overhead approach was the principal path studied (i.e., one in which the aircraft crossed over the runway at

a 90° angle heading east at an altitude of 550 m). At about 1800 m east of the runway centerline it intercepted the helix and descended along it, making a total turn, to the right, of 270°. The turn was completed at an altitude of 100 m where the aircraft intercepted the straight-in approach. At this time, it was about 1900 m from the touchdown point on the runway. The plane continued to descend until at a 12-m altitude, the onset of the flare maneuver, the simulation was terminated. The effectiveness of the control system was tested in the nonlinear simulation by introducing initial errors in the states, cross-winds, and uncertainties in the aerodynamics of the aircraft.

SYMBOLS

$A, A(t)$	state-coefficient matrix (6×6) in linearized equations of motion
$B, B(t)$	control-coefficient matrix (6×3) in linearized equations of motion
C_D	total drag coefficient
$C_{D,o}$	drag coefficient for zero lift
C_L	total lift coefficient
C_{L_α}	$= \partial C_L / \partial \alpha$, rad^{-1}
D	aerodynamic drag force, N
$\bar{f}, \bar{f}(\bar{x}, \bar{u})$	derivative of the state vector $\bar{x}$ (6×1)
$\bar{f}_1$	vector function (3×1) used in determining nominal open-loop control for equilibrium
g	gravitational force per unit mass, 9.80 m/sec^2
h	altitude (-z), m
H	Hamiltonian of linearized system
J	cost functional (performance index)

$K, K(t)$	feedback-gain matrix (3×6)
$K_{i,j}$	i,j element of K
L	aerodynamic lift force, N
m	mass of aircraft, kg
M	weighting matrix (6×6) on terminal-state variations
$\overline{p}, \overline{p}(t)$	vector (6×1) of costates
q	dynamic pressure, N/m^2
Q	weighting matrix (6×6) on state variations
r	radius of helix, m
R	weighting matrix (3×3) on control variations
S	reference wing area of aircraft, m^2
$S_1, S_1(t)$	matrix (6×6) relating the costates to the states in equation (26), solution of the time-varying matrix Riccati equation
t	time, independent variable, sec
T	total engine thrust. N
T/m	thrust to mass ratio, m/sec^2
T_γ	orthogonal transformation (3×3) through the angle γ
T_ϕ	orthogonal transformation (3×3) through the angle ϕ
T_ψ	orthogonal transformation (3×3) through the angle ψ
$\overline{u}$	control vector (3×1), $[\alpha \quad \phi \quad T/m]^T$

V	magnitude of the velocity vector with respect to the inertial axis system, m/sec
$\overline{V}$	velocity vector (3×1) resolved along rotating axes system
V_W	scalar magnitude of crosswinds, m/sec or knots
x	displacement of aircraft in the north-south direction relative to the origin of the fixed axes system, m
$\overline{x}$	state vector (6×1) of the system, $[x \quad y \quad z \quad V \quad \gamma \quad \psi]^T$
X,Y,Z	inertial axis system
X',Y',Z'	rotating axis system
y	displacement of aircraft in the east-west direction relative to the origin of the fixed axes system, m
z	vertical displacement of aircraft relative to the origin of the fixed axes system, m
$\dot{z}$	sink rate, m/sec
Z,Z(t)	state coefficient matrix (12×12) in equation (23b)
α	angle of attack, deg
α_o	angle of attack for zero lift, deg
γ	flight-path angle, rad or deg
$\overline{\delta u}$	variation from nominal control vector (3×1)
$\overline{\delta x}$	variation from nominal state vector (6×1)
$\delta\alpha_R, \delta\phi_R, \delta(T/m)_R$	symbols used in defining the diagonal elements of the R weighting matrix

$\left.\begin{matrix}\delta x_M, \delta y_M \\ \delta z_M, \delta V_M \\ \delta \gamma_M, \delta \psi_M\end{matrix}\right\}$ symbols used in defining the diagonal elements of the M weighting matrix

$\left.\begin{matrix}\delta x_Q, \delta y_Q \\ \delta z_Q, \delta V_Q \\ \delta \gamma_Q, \delta \psi_Q\end{matrix}\right\}$ symbols used in defining the diagonal elements of the Q weighting matrix

η aerodynamic efficiency factor in equations (6)

$\rho, \rho(h)$ density of air, kg/m^3

ϕ aircraft roll angle, rad or deg

ψ aircraft track angle, rad or deg

ψ_w direction of wind, rad or deg

$\overline{\omega}$ rotation vector of aircraft (3×1) resolved along rotating axis system

$\Omega, \Omega(t,h)$ transition matrix (12×12) for the combined system of states and costates in equation (24)

$\Omega_{i,j}$ submatrices (6×6) of Ω

Subscripts:

0 initial value

f final value

N nominal value

SI nominal value when the aircraft executes roll-out maneuver

Operators:

$\bar{a} \times \bar{b}$	cross product of a and b
U[a,b]	uniformly distributed random variable with range (a,b)
$[\ ]^{-1}$	inverse of matrix
$[\ ]^T$	transpose of matrix or vector

A dot over a variable denotes the derivative with respect to time.

ANALYSIS

The purpose of this section is to present the mathematics involved in simulating the aircraft and in implementing the feedback control law. As illustrated in figure 1, the aircraft is modeled by a set of six nonlinear ordinary differential equations represented by the single vector equation

$$\dot{\bar{x}} = \bar{f}(\bar{x},\bar{u}) \tag{1}$$

This set of equations was integrated numerically using a fixed-step fourth-order Runge Kutta algorithm. The feedback control law used in this study requires that the nominal state trajectories $\bar{x}_N$, the nominal control time histories $\bar{u}_N$, and the feedback gain matrix K be stored in an on-board computer. However, it will be shown that by choosing particular nominal trajectories, the vector $\bar{u}_N$ changes only twice, and the vector $\bar{x}_N$ is a simply computed analytic vector function of time. This eliminates some of the on-board storage requirements and makes the control system simpler and more flexible.

As simulated, the aircraft has six state variables and three control inputs defined as

$$\bar{x} = [x \quad y \quad z \quad V \quad \gamma \quad \psi]^T$$

$$\bar{u} = [\alpha \quad \phi \quad T/m]^T$$

The state vector $\bar{x}$ is made up of the variables x, y, and z describing the aircraft's position; V, its inertial speed; γ, its flight-path angle; and ψ, its track angle. The control vector $\bar{u}$ is made up of the angle of attack α, the roll angle ϕ, and the ratio of

engine thrust to aircraft mass T/m. The two perturbation vectors $\overline{\delta x}$ and $\overline{\delta u}$, shown in figure 1, are defined as

$$\overline{\delta x} = \bar{x} - \bar{x}_N$$

$$\overline{\delta u} = \bar{u} - \bar{u}_N$$

However, in practice, $\overline{\delta u}$ is computed as:

$$\overline{\delta u} = K\overline{\delta x} \tag{2}$$

where K is a 3×6 time-varying gain matrix. This gain matrix is the solution of the regulator problem which results from linearizing equation (1) about the nominal flight path and control vector, and it is precomputed for a particular nominal flight path. This linearization yields:

$$\dot{\overline{\delta x}} = A(t)\overline{\delta x} + B(t)\overline{\delta u} = [A(t) + B(t)K(t)]\overline{\delta x} \tag{3}$$

where $A(t) = \partial \bar{f}/\partial \bar{x}$ evaluated at $\bar{x} = \bar{x}_N$ and $\bar{u} = \bar{u}_N$, $B(t) = \partial \bar{f}/\partial \bar{u}$ evaluated at $\bar{x} = \bar{x}_N$ and $\bar{u} = \bar{u}_N$, $A(t)$ is a 6×6 matrix, and $B(t)$ is a 6×3 matrix. A statement of the regulator problem is then to find K in equations (2) and (3) which minimizes deviations of the states and controls from their nominal values.

More formally, the problem is to determine K which minimizes the quadratic performance index J given by

$$J = \frac{1}{2}\overline{\delta x}^T(t_f)M\overline{\delta x}(t_f) + \frac{1}{2}\int_0^{t_f}\left[\overline{\delta x}(t)^T Q\overline{\delta x}(t) + \overline{\delta u}(t)^T R\overline{\delta u}(t)\right] dt \tag{4}$$

subject to the constraints of equation (3) and where M, Q, and R are weighting matrices.

Equations of Motion

The inertial axis system illustrated in figure 2 has its origin at the glide-path intercept point on the runway. The X-axis is parallel to the runway and is positive in the direction of landing. The Y-axis is horizontal, perpendicular to the X-axis and is positive to the right. The vertical Z-axis is perpendicular to both X and Y, and is positive downward. The aircraft is treated as a point mass, subject to the forces of gravity, engine thrust, and aerodynamic lift and drag. The rotating axis system associ-

ated with the aircraft is chosen such that its X'-axis is always alined with the aircraft's velocity vector. Two Euler angle transformations relate the inertial axis system to the rotating axis system. They are

$$T_\psi = \begin{bmatrix} \cos\psi & \sin\psi & 0 \\ -\sin\psi & \cos\psi & 0 \\ 0 & 0 & 1 \end{bmatrix}$$

and

$$T_\gamma = \begin{bmatrix} \cos\gamma & 0 & \sin\gamma \\ 0 & 1 & 0 \\ -\sin\gamma & 0 & \cos\gamma \end{bmatrix}$$

These rotations are shown in figure 2. This axis system does not roll with the aircraft. Therefore, the Y'-axis remains horizontal and the Z'-axis stays in a vertical plane with the velocity vector. The rotation vector resolved along the rotating axis system is

$$\overline{\omega} = [\dot{\psi}\sin\gamma \quad -\dot{\gamma} \quad \dot{\psi}\cos\gamma]^T$$

and the velocity vector is

$$\overline{V} = [V \quad 0 \quad 0]^T$$

The forces acting on the aircraft resolved along the rotating axes are

$$\text{Drag} = [-D \quad 0 \quad 0]^T$$

$$\text{Thrust} = T_\phi[T\cos\alpha \quad 0 \quad -T\sin\alpha]^T$$

$$\text{Gravity} = T_\gamma T_\psi[0 \quad 0 \quad mg]^T$$

$$\text{Lift} = T_\phi[0 \quad 0 \quad -L]^T$$

where

$$T_\phi = \begin{bmatrix} 1 & 0 & 0 \\ 0 & \cos\phi & -\sin\phi \\ 0 & \sin\phi & \cos\phi \end{bmatrix}$$

The lift force is perpendicular to the velocity and rolls with the aircraft. The transformation T_ϕ resolves this force along the Y'- and Z'-rotating axes. The angle of attack α is defined as the angle between the velocity vector and the thrust vector of the aircraft. The dynamics of the aircraft are then described by equating the change in linear momentum to the sum of the applied forces

$$m(\dot{\overline{V}} + \overline{\omega} \times \overline{V}) = \text{Drag} + \text{Thrust} + \text{Gravity} + \text{Lift}$$

or

$$m\begin{bmatrix} \dot{V} \\ 0 \\ 0 \end{bmatrix} + m\begin{bmatrix} 0 \\ V\dot{\psi}\cos\gamma \\ V\dot{\gamma} \end{bmatrix} = \begin{bmatrix} -D \\ 0 \\ 0 \end{bmatrix} + \begin{bmatrix} T\cos\alpha \\ T\sin\alpha\sin\phi \\ -T\sin\alpha\cos\phi \end{bmatrix} + \begin{bmatrix} mg\sin\gamma \\ 0 \\ mg\cos\gamma \end{bmatrix} + \begin{bmatrix} 0 \\ L\sin\phi \\ -L\cos\phi \end{bmatrix}$$

To facilitate integration of these equations, they are written with the derivatives of the states V, ψ, and γ on the left-hand side. These three equations are combined with three kinematic relations which resolve the velocity along the X-, Y-, and Z-inertial axes

$$\begin{bmatrix} \dot{x} \\ \dot{y} \\ \dot{z} \end{bmatrix} = \left[T_\gamma T_\psi\right]^{-1} \begin{bmatrix} V \\ 0 \\ 0 \end{bmatrix}$$

The six equations of state are then

$$\dot{x} = V\cos\gamma\cos\psi \tag{5a}$$

$$\dot{y} = V\cos\gamma\sin\psi \tag{5b}$$

$$\dot{z} = V\sin\gamma \tag{5c}$$

$$\dot{V} = \frac{-D}{m} + \frac{T}{m} \cos \alpha + g \sin \gamma \tag{5d}$$

$$\dot{\gamma} = \frac{g}{V} \cos \gamma - \frac{L}{mV} \cos \phi - \frac{T}{mV} \sin \alpha \cos \phi \tag{5e}$$

$$\dot{\psi} = \frac{(L + T \sin \alpha) \sin \phi}{mV \cos \gamma} \tag{5f}$$

Equations (5) are the expanded form of equation (1).

Aerodynamics and Aircraft Parameters

The aircraft simulated in this study is a small two-engined transport airplane designed primarily to operate from short runways over relatively short distances. It is described in references 9 and 10.

The equations for the lift and drag forces are

$$L = qSC_L$$

$$D = qSC_D$$

where S is the wing reference area and C_L and C_D are the coefficients of lift and drag, respectively, and q is dynamic pressure which are defined as

$$\left.\begin{aligned} C_L &= C_{L_\alpha}(\alpha - \alpha_o)\frac{\pi}{180} \\ C_D &= C_{D,o} + \eta C_L^{\,2} \\ q &= \frac{1}{2}\rho V^2 \end{aligned}\right\} \tag{6}$$

where a parabolic drag polar has been assumed. This assumption is not restrictive for the range of speed and angle of attack employed in this study. Air density ρ was approximated by the following equation taken from reference 8.

$$\rho = 1.22\left[1 - (2.257 \times 10^{-5})h\right]^{4.255} \tag{7}$$

This proved to be a very good approximation to the standard atmospheric density of reference 11. The airplane was configured with the landing gear down and the flaps deployed at 40°. The parameters of equations (6) $\left(C_{L_\alpha},\ \alpha_o,\ C_{D,o}, \text{ and } \eta\right)$ were chosen to fit data on C_L and C_D provided by the manufacturer for this configuration. The parameters of the airplane are listed in table 1.

Nominal Flight Paths

Linear regulator theory does not in any way restrict the choice of nominal flight path. However, practical considerations including ease of implementation do suggest certain types of landing approaches. If a path on which the derivatives of velocity and flight-path angle are identically zero is chosen, then the nominal state trajectories can be expressed as simple analytic functions of time. In which case, much less on-board computer memory is needed to store the path. Before examining the helical landing approach, first look at the conventional 3°, nondecelerating, straight-in approach. A mathematical description of this path is

$$\dot{\bar{x}} = \begin{bmatrix} V_0 \cos\gamma_0 & 0 & V_0 \sin\gamma_0 & 0 & 0 & 0 \end{bmatrix}^T$$

$$\bar{x}(0) = \begin{bmatrix} x_0 & 0 & z_0 & V_0 & \gamma_0 & 0 \end{bmatrix}^T$$

As the aircraft approaches the ground, it leaves this quasi-steady condition and flares in order to touch down smoothly. This path calls for constant control inputs varying only to offset atmospheric disturbances. Because of its simplicity, it can be easily implemented.

In order to relieve airport noise problems and to decrease traffic congestion in the neighborhood of the airport, various other approaches have been proposed and are being tested. These include the steeper 6°, nondecelerating, straight-in approach and a combination of the 6° and 3° approach. The method proposed in this paper is a constant-control helical approach. All other constant-control paths are special cases of this generalization. That is, the nominal path is descent along a helix from some initial altitude. The centerline of the runway is tangent to the helix, and at some specified lower altitude, the aircraft follows this tangent into a straight-in approach. By making the assumption that atmospheric density is constant over the range of altitude considered, this path calls for fixed controls during the helical descent, and fixed (but different) control inputs during the straight-in portion. The variation in atmospheric density in this range of altitude (0 to 700 m) is about 4 percent. The assumption of constant density is made during calculations of nominal path, nominal control inputs, and feedback gains. During the simu-

lated flights, using the closed-loop control system, atmospheric density is allowed to vary according to equation (7). The small error introduced by this assumption was nulled out by the control system as though it were an external disturbance. A more formal description of the nominal path is

$$\dot{\bar{x}} = \begin{bmatrix} V_0 \cos\gamma_0 \cos\psi \\ V_0 \cos\gamma_0 \sin\psi \\ V_0 \sin\gamma_0 \\ 0 \\ 0 \\ \dot{\psi}_0 \end{bmatrix} \qquad \bar{x}(0) = \begin{bmatrix} x_0 \\ y_0 \\ z_0 \\ V_0 \\ \gamma_0 \\ \psi_0 \end{bmatrix} \tag{8}$$

for the altitude range

$$-z_0 \geqq h \geqq -z_{SI}$$

where $-z_{SI}$ is the altitude at which the aircraft rolls into the straight-in approach. The parameters z_0, z_{SI}, V_0, γ_0, and ψ_0 are chosen with some degree of latitude and they essentially determine the nominal flight path. The last three parameters $(x_0,\ y_0,$ and $\dot{\psi}_0)$ are functions of the former and are chosen such that x, y, and ψ have the desired values when z equals z_{SI}. The subscript SI will be used to specify the value of a state when z equals z_{SI}. Because the origin of the axis system is at the glide-path intercept point on the runway, the desired values of ψ_{SI} and y_{SI} are zero. In order to determine x_{SI}, it is necessary to look at the nominal path after it starts the straight-in approach. Its description is

$$\left.\begin{aligned} \dot{\bar{x}} &= \begin{bmatrix} V_0 \cos\gamma_0 & 0 & V_0 \sin\gamma_0 & 0 & 0 & 0 \end{bmatrix}^T \\ \bar{x}(t_{SI}) &= \begin{bmatrix} x_{SI} & 0 & z_{SI} & V_0 & \gamma_0 & 0 \end{bmatrix}^T \end{aligned}\right\} \tag{9}$$

During the straight-in part of the flight $\dot{x}$ and $\dot{z}$ are constant and consequently,

$$\frac{dx}{dz} = \frac{dx/dt}{dz/dt} = \cot\gamma_0$$

is constant. In order to touch down at the origin, x_{SI} and z_{SI} must be related by

$$x_{SI} = z_{SI} \frac{dx}{dz}$$

or

$$x_{SI} = \frac{z_{SI}}{\tan \gamma_0} \tag{10}$$

Also, during the helical descent, the rate of turn $\dot{\psi}$ and the rate of descent $\dot{z}$ are constant. In order to have the aircraft flying in the correct direction ($\psi = 2\pi$) when z equals z_{SI}, it is necessary that

$$\frac{d\psi}{dz} = \frac{2\pi - \psi_0}{z_{SI} - z_0} \tag{11}$$

and since

$$\frac{d\psi}{dt} = \frac{d\psi}{dz} \frac{dz}{dt}$$

it follows that

$$\dot{\psi}_0 = \left(\frac{2\pi - \psi_0}{z_{SI} - z_0}\right) V_0 \sin \gamma_0 \tag{12}$$

The axis of the helix is vertical with origin at

$$(x,y) = (x_{SI}, r)$$

where the radius r is given by

$$r = \frac{1}{\tan \gamma_0 \frac{d\psi}{dz}} \tag{13}$$

and through geometrical considerations

$$x_0 = x_{SI} + r \sin \psi_0 \tag{14}$$

$$y_0 = r(1 - \cos \psi_0) \tag{15}$$

A short example may clarify these computations (see fig. 3, flight path 2). Let the landing direction be north ($\psi = 2\pi$) and the aircraft's original heading (t = 0) be east ($\psi_0 = \pi/2$). The velocity is 62 m/sec and the flight-path angle is 6^o or $6\pi/180$ rad. Initial altitude is 550 m. The aircraft descends along a helical path to a 100-m altitude and then down a straight path to the runway. In this example,

$$z_0 = -550 \text{ m}$$

$$z_{SI} = -100 \text{ m}$$

$$V_0 = 62 \text{ m/sec}$$

$$\gamma_0 = \frac{6\pi}{180}$$

$$\psi_0 = \frac{\pi}{2}$$

$$x_{SI} = \frac{z_{SI}}{\tan \gamma_0} = -\frac{100}{\tan \frac{6\pi}{180}} \approx -951 \text{ m}$$

$$\frac{d\psi}{dz} = \frac{2\pi - \psi_0}{z_{SI} - z_0} = \frac{3\pi}{2(-100 + 550)} = \frac{3\pi}{900} \approx 0.010 \text{ rad/m}$$

$$\dot{\psi}_0 = \frac{d\psi}{dz}\frac{dz}{dt} = \frac{3\pi}{900} 62 \sin \frac{6\pi}{180} \approx 0.068 \text{ rad/sec}$$

$$r = \frac{1}{\tan \gamma_0 \frac{d\psi}{dz}} = \frac{900}{3\pi \tan \frac{6\pi}{180}} \approx 909 \text{ m}$$

$$x_0 = x_{SI} + r \sin \psi_0 \approx -951 + 909 \sin \frac{\pi}{2} \approx -43 \text{ m}$$

$$y_0 = r(1 - \cos \psi_0) = r \approx 909 \text{ m}$$

Integration of equations (8) gives the following state trajectories along the helix.

$$\bar{x} = \begin{bmatrix} x_0 \\ y_0 \\ z_0 \\ V_0 \\ \gamma_0 \\ \psi_0 \end{bmatrix} + \begin{bmatrix} \left(\frac{V_0 \cos \gamma_0}{\dot{\psi}_0}\right)(\sin \psi - \sin \psi_0) \\ \left(\frac{V_0 \cos \gamma_0}{\dot{\psi}_0}\right)(\cos \psi_0 - \cos \psi) \\ (V_0 \sin \gamma_0)t \\ 0 \\ 0 \\ \dot{\psi}_0 t \end{bmatrix} \tag{16}$$

Likewise, integration of equations (9) yields the state trajectories along the straight portion of the flight path

$$\bar{x} = \begin{bmatrix} x_{SI} \\ 0 \\ z_{SI} \\ V_0 \\ \gamma_0 \\ 0 \end{bmatrix} + \begin{bmatrix} V_0 \cos \gamma_0 \\ 0 \\ V_0 \sin \gamma_0 \\ 0 \\ 0 \\ 0 \end{bmatrix} (t - t_{SI}) \tag{17}$$

The time for the wings-level maneuver t_{SI} is given by

$$t_{SI} = \frac{z_{SI} - z_0}{V_0 \sin \gamma_0} \tag{18}$$

In summary, for a helical approach there is no need to integrate and store the equations of motion. Given a particular input parameter set $(z_0, z_{SI}, V_0, \gamma_0, \psi_0)$ equations (16) and (17) yield the value of the states at any time. Five secondary parameters $(x_{SI}, \dot{\psi}_0, x_0, y_0, t_{SI})$ necessary to evaluate equations (16) and (17) are given as functions of the input parameters by equations (10) to (15) and equation (18).

Nominal Control Inputs

After specifying this particular class of nominal flight paths, it is necessary to solve for the appropriate open-loop control. Since, as has been stated earlier in equations (8) and (9),

$$\dot{V} = \dot{\gamma} = 0$$

$$\dot{\psi} = \dot{\psi}_0 \qquad \text{for} \quad h \geq -z_{SI}$$

$$\dot{\psi} = 0 \qquad \text{for} \quad h \leq -z_{SI}$$

$\bar{u}$ is a constant vector on the spiral and a second constant on the straight-in portion. In order to make equations (5) agree with equations (8), the following equations must be satisfied:

$$\left.\begin{aligned} &\frac{D_N}{m} - \frac{T}{m}\cos\alpha - g\sin\gamma_0 = 0 \\ &\frac{T}{mV_0}\sin\alpha\cos\phi - \frac{g}{V_0}\cos\gamma_0 + \frac{L_N}{mV_0}\cos\phi = 0 \\ &\dot{\psi}_0 - \frac{(L_N + T\sin\alpha)\sin\phi}{mV_0\cos\gamma_0} = 0 \end{aligned}\right\} \qquad (19)$$

In these equations,

$$L_N = q_N S C_L$$

$$D_N = q_N S C_D$$

where

$$q_N = \frac{1}{2}\rho_N V_0^2$$

and C_L and C_D are defined in equations (6). Using the assumption of constant air density discussed earlier, an intermediate value of altitude h_N is chosen, and ρ_N is computed using equation (7). The open-loop control

$$\bar{u} = [\alpha \quad \phi \quad T/m]^T$$

which is the solution of equations (19), is not unique and these equations have no closed-form solution. Equations (19) are of the form

$$\bar{f}_1(\bar{u}) = 0$$

and it was solved by the Newton-Raphson iterative method described in reference 12. This method usually requires the Jacobian matrix which is given by

$$\frac{\partial \bar{f}_1}{\partial \bar{u}} = \begin{bmatrix} \dfrac{\partial D_N}{\partial \alpha} + T \sin \alpha}{m} & 0 & -\cos \alpha \\ \dfrac{\left(T \cos \alpha + \dfrac{\partial L_N}{\partial \alpha}\right) \cos \phi}{mV_0} & \dfrac{-\left(L_N + T \sin \alpha\right) \sin \phi}{mV_0} & \dfrac{\cos \phi \sin \alpha}{V_0} \\ \dfrac{-\left(T \cos \alpha + \dfrac{\partial L}{\partial \alpha}\right) \sin \phi}{mV_0 \cos \gamma_0} & \dfrac{-\left(L_N + T \sin \alpha\right) \cos \phi}{mV_0 \cos \gamma_0} & \dfrac{-\sin \alpha \sin \phi}{V_0 \cos \gamma_0} \end{bmatrix}$$

where

$$\frac{\partial L_N}{\partial \alpha} = q_N S \frac{\pi}{180} C_{L_\alpha}$$

and

$$\frac{\partial D_N}{\partial \alpha} = 2 q_N S \left(\frac{\pi}{180}\right)^2 C_{L_\alpha}^2 \eta (\alpha - \alpha_0)$$

The possibility always exists that this algorithm will not converge at all or will converge to an undesirable value of $\bar{u}$. Therefore, the solution must be examined subjectively before being accepted. A practical way to avoid this problem is to start the iterative procedure close to the desired final solution. A suggested method of doing this

is to make the assumption that engine thrust is alined with the velocity vector of the aircraft. With this assumption, which is in error by the size of the angle of attack, equations (19) become

$$\frac{D_N}{m} - \frac{T}{m} - g \sin \gamma_0 = 0$$

$$-\frac{g}{V_0} \cos \gamma_0 + \frac{L_N}{mV_0} \cos \phi = 0$$

$$\dot{\psi}_0 - \frac{L_N \sin \phi}{mV_0 \cos \gamma_0} = 0$$

These equations have the following closed-form solution which can be used as a starting point in the Newton-Raphson algorithm. The solution is

$$\left.\begin{aligned} \phi &= \tan^{-1} \frac{V_0 \dot{\psi}_0}{g} \\ \alpha &= \alpha_0 + \frac{\frac{180}{\pi} mg \cos \gamma_0}{q_N S C_{L_\alpha} \cos \phi} \\ \frac{T}{m} &= \frac{D_N}{m} - g \sin \gamma_0 \end{aligned}\right\} \tag{20}$$

In order to solve for the open-loop controls for the straight-in portion of the nominal flight path, the following equations must be satisfied:

$$\left.\begin{aligned} \frac{D_N}{m} - \frac{T}{m} \cos \alpha - g \sin \gamma_0 &= 0 \\ \frac{T}{mV_0} \sin \alpha - \frac{g}{V_0} \cos \gamma_0 + \frac{L_N}{mV_0} &= 0 \end{aligned}\right\} \tag{21}$$

Again, the Newton-Raphson algorithm is used to solve the two equations for α and T/m. The roll angle ϕ, of course, is zero. Using the same assumption as before that thrust and velocity are codirectional, the following equations can be used to start the iterative procedure.

$$\left.\begin{aligned} \alpha &= \frac{180}{\pi}\frac{mg\cos\gamma_0}{qSC_{L_\alpha}} + \alpha_0 \\ \frac{T}{m} &= \frac{D_N}{m} - g\sin\gamma_0 \end{aligned}\right\} \tag{22}$$

Notice that D_N in equations (20) will have a different numerical value than D_N in equations (21). These equations used for starting the Newton-Raphson iteration procedure yield values which are very close to the final values.

Feedback Control Gains

The purpose of this section is to outline the solution of the linear regulator problem. References 1 to 5 all are concerned, in part, with this problem. A statement of the problem is given by equations (1), (3), and (4), which are repeated here for convenience.

$$\dot{\bar{x}} = \bar{f}(\bar{x},\bar{u})$$

$$\dot{\overline{\delta x}} = A(t)\overline{\delta x} + B(t)\overline{\delta u} = \left[A(t) + B(t)K(t)\right]\overline{\delta x}$$

$$J = \frac{1}{2}\overline{\delta x}^T(t_f)M\overline{\delta x}(t_f) + \frac{1}{2}\int_0^{t_f}\left[\overline{\delta x}(t)^T Q\overline{\delta x}(t) + \overline{\delta u}(t)^T R\overline{\delta u}(t)\right]dt$$

$A(t)$ and $B(t)$ are defined as

$$A = \frac{\partial \bar{f}}{\partial \bar{x}} \qquad\qquad B = \frac{\partial \bar{f}}{\partial \bar{u}}$$

and M, Q, and R are weighting matrices which must be selected by the control-system designer. The problem is to find the matrix K in equation (3) which minimizes the quadratic performance index of equation (4). As shown in the references, the state equations are combined with the costate equations to form the system:

$$\begin{bmatrix} \dot{\overline{\delta x}} \\ \dot{\bar{p}} \end{bmatrix} = \begin{bmatrix} A & -BR^{-1}B^T \\ -Q & -A^T \end{bmatrix}\begin{bmatrix} \overline{\delta x} \\ \bar{p} \end{bmatrix} \tag{23a}$$

where $\bar{p}$ is the vector of costates.[1] Equation (23a) can be rewritten in the form

$$\begin{bmatrix} \dot{\overline{\delta x}} \\ \dot{\bar{p}} \end{bmatrix} = Z \begin{bmatrix} \overline{\delta x} \\ \bar{p} \end{bmatrix} \tag{23b}$$

and if we assume that Z is constant over a small interval of time Δt then we can write the transition equation of the system as

$$\begin{bmatrix} \overline{\delta x}(t + \Delta t) \\ \bar{p}(t + \Delta t) \end{bmatrix} = \Omega(t, \Delta t) \begin{bmatrix} \overline{\delta x}(t) \\ \bar{p}(t) \end{bmatrix} \tag{24}$$

where

$$\Omega(t, \Delta t) = e^{Z(t)\ \Delta t} = \begin{bmatrix} \Omega_{11} & \Omega_{12} \\ \Omega_{21} & \Omega_{22} \end{bmatrix} \tag{25}$$

It is further shown that the costates are linearly related to the states; that is,

$$\bar{p}(t) = S_1 \overline{\delta x}(t) \tag{26}$$

and that the final condition on S_1 is given by

$$S_1(t_f) = M \tag{27}$$

Combining equations (24), (25), and (26) yields a transition equation for S_1

$$\begin{bmatrix} \overline{\delta x}(t + \Delta t) \\ S_1(t + \Delta t)\overline{\delta x}(t + \Delta t) \end{bmatrix} = \Omega(t, \Delta t) \begin{bmatrix} \overline{\delta x}(t) \\ S_1(t)\overline{\delta x}(t) \end{bmatrix}$$

$$S_1(t + \Delta t)\left[\Omega_{11} + \Omega_{12} S_1(t)\right] \overline{\delta x}(t) = \left[\Omega_{21} + \Omega_{22} S_1\right] \overline{\delta x}(t)$$

[1] Reference 2 shows that M, Q, and R must be symmetric; that M and Q must be at least positive semidefinite; and that R must be positive definite.

or

$$S_1(t + \Delta t) = \left[\Omega_{21} + \Omega_{22}S_1(t)\right]\left[\Omega_{11} + \Omega_{12}S_1(t)\right]^{-1} \tag{28}$$

Reference 2 proves that this inverse does exist. A comprehensive development of equation (28) can be found in chapter 7 of reference 13.

Using the difference equation (28) with the final value of the matrix S_1 given by equation (27), we can proceed backward in time and obtain S_1 for all t in the range (t_0,t_f). At each point in time, it is necessary to compute $\Omega(t,\Delta t)$ as a function of $A(t)$, $B(t)$, R, and Q, using equations (23) to (25). The gain matrix $K(t)$ is obtained by the following relationship:

$$\overline{\delta u} = -R^{-1}B^T S_1 \overline{\delta x}(t)$$

or

$$K(t) = -R^{-1}B^T S_1 \tag{29}$$

Implementation

The landing-approach guidance scheme proposed in this paper would be implemented in the following manner:

(1) For a particular nominal flight path, the control-system designer, after extensive analysis and testing, chooses weighting matrices M, Q, and R for the performance index in equation (4).

(2) The state trajectories on the nominal flight path are computed using equations (10) to (18).

(3) The nominal open-loop control inputs are computed using the Newton-Raphson algorithm to solve equations (19) and (21). This iterative procedure is started with the values given in equations (20) and (22), respectively.

(4) The Jacobian matrices $A(t)$ and $B(t)$ used in equation (3) are computed according to equations (A1) and (A2) in the appendix. Equation (3) represents the linearization of equation (1) about the nominal trajectory and control.

(5) The feedback gain matrix K is computed as a function of time using equations (23) to (29).

(6) In the computer aboard the aircraft are stored the time histories of the nominal flight path, the nominal control inputs, and the feedback gains. Alternatively, the algorithm (eqs. (16) and (17)) which computes the state trajectories is stored.

(7) The aircraft, or simulated aircraft, is flown into a window (i.e., a region of state space which is "close" to the initial states of the nominal flight path).

(8) When the plane enters the window, it is switched onto the automatic landing system. It is assumed that the aircraft is receiving the necessary position data from the ground-based airport landing system and receives control-surface positions from transducers. This is considered time zero with respect to the nominal path.

(9) The control system nulls the state errors and brings the aircraft onto the nominal flight path before reaching the decision altitude.

RESULTS AND DISCUSSION

Flight Paths

In this study, the control system was tested along seven different nominal flight paths which are described in table 2. The paths differed in initial altitude, initial heading angle, and in angle of descent. Flight paths 1, 2, and 3 are depicted in figure 3.

Flight path 1 is the easiest path to fly because its initial altitude is the highest and there is more time to null out initial errors in the state variables. Conversely, flight path 3 is the most difficult since its initial altitude is 150 m below flight path 2 and 300 m below flight path 1. The aircraft makes a descending turn to the right of 360°, 270°, and 180° for flight paths 1, 2, and 3, respectively, at which point it is headed north toward the runway. At this position (roll out) on the path, the aircraft is at a 100-m altitude and it rolls to a wing-level attitude. It then descends in a straight line toward the runway. The simulation terminated at initiation of flare where off-nominal errors were recorded.

Flight paths 1A, 2A, and 3A had the same initial altitude and heading, respectively, as flight paths 1, 2, and 3. However, they had a descent angle of 6° rather than 3°. These flight paths require more control than the first three and less time is available to null off-nominal errors. The rate of descent and roll angle are about doubled and the turning radius and flight time are about halved. The rollout altitude was maintained at 100 m.

Flight path 3B is a variation of 3A. The initial altitude and rollout altitude were raised 100 m. This had the effect of moving the helix back from the runway and about doubling the time spent on the straight-in portion of the path.

Design Considerations

The control task presented here differs from conventional landing-approach schemes in that errors are taken with respect to a moving point in state space rather than a fixed line. Thus, even if the aircraft was flying on the correct helical path with the correct attitude, the fact that it was late or early in time would indicate to the control system that there were state errors; in this context, the proposed guidance scheme can be considered four-dimensional. At crowded airports, more precise control of time sequencing should prove advantageous.

Because the feedback gain matrix K is computed automatically, the designer's job is to choose the weighting matrices M, Q, and R of equation (4) and then to evaluate the subsequent performance of the control system. In fact, this becomes an iterative procedure where the designer is trying to find an optimum set of weighting parameters. This task is not trivial, but by using diagonal weighting matrices, a functional relationship between their elements and the subsequent performance can be established.

The control system was required to null out initial errors in the states, and to offset the effects of steady crosswinds. It was also desired that it not be sensitive to normal changes in the atmosphere and uncertainties in the aircraft's aerodynamics. Wind gusts and sensor noise were not considered in this study. Large initial state errors tend to demand large rapid control motions. In order to avoid this, state errors are weighted less by reducing the elements of Q and control excursions are weighted more by increasing the elements of R.[2] However, the performance index does not include control rates and the R matrix influences the time integral rather than the magnitude of control excursion squared. Therefore, it is not unusual to get large control excursions for relatively short time with consequent high control rates. If the Q and R matrices are well chosen, the control system will null out the initial errors slowly in a manner which will cause no passenger discomfort. As the aircraft approaches the touchdown point, the influence of the M matrix tightens up the control and acceptable values of final state errors can be achieved.

This approach worked fine until the aircraft was subjected to a crosswind. It then became apparent that control in crosswinds was a much more stringent requirement and that a tighter control was necessary. To reconcile the two requirements (wide bandwidth control for crosswinds and narrow bandwidth control for large initial errors) two approaches were taken. First, high gains were used, but rate and position limits were placed on the controls. This led to undesirable oscillatory behavior, and in some cases, instability. The rate limit on angle of attack seemed to be particularly troublesome. The second approach was to make the elements of Q and R time varying. In this

[2]The initial choice of the M, Q, and R matrices was made following the suggestion on page 149 of reference 3.

method, the feedback gains are low initially, while the state errors are large. While the large errors are being nulled, the feedback gains are gradually increased and the system is reasonably tight when it approaches touchdown. This second method works well except that roll rate became excessive when the aircraft rolled out of its turn. This maneuver occurs at a 100-m altitude when high feedback gains are desirable. This problem was circumvented by imposing a rate limit on roll. The values of Q, R, and M which were finally settled upon are:

$$Q = \frac{1}{2t_f}\begin{bmatrix} \delta x_Q^{-2} & 0 & 0 & 0 & 0 & 0 \\ 0 & \delta y_Q^{-2} & 0 & 0 & 0 & 0 \\ 0 & 0 & \delta z_Q^{-2} & 0 & 0 & 0 \\ 0 & 0 & 0 & \delta V_Q^{-2} & 0 & 0 \\ 0 & 0 & 0 & 0 & \delta\gamma_Q^{-2} & 0 \\ 0 & 0 & 0 & 0 & 0 & \delta\psi_Q^{-2} \end{bmatrix}$$

$$R = \frac{1}{2t_f}\begin{bmatrix} \delta\alpha_R^{-2} & 0 & 0 \\ 0 & \delta\phi_R^{-2} & 0 \\ 0 & 0 & \delta(T/m)_R^{-2} \end{bmatrix}$$

$$M = \begin{bmatrix} \delta x_M^{-2} & 0 & 0 & 0 & 0 & 0 \\ 0 & \delta y_M^{-2} & 0 & 0 & 0 & 0 \\ 0 & 0 & \delta z_M^{-2} & 0 & 0 & 0 \\ 0 & 0 & 0 & \delta V_M^{-2} & 0 & 0 \\ 0 & 0 & 0 & 0 & \delta\gamma_M^{-2} & 0 \\ 0 & 0 & 0 & 0 & 0 & \delta\psi_M^{-2} \end{bmatrix}$$

where the value of the elements are given by

$$\left.\begin{aligned} \delta x_Q &= 140 - 85\,\frac{t}{t_f} \\ \delta y_Q &= 140 - 131\,\frac{t}{t_f} \\ \delta z_Q &= 31 - 26\,\frac{t}{t_f} \\ \delta V_Q &= 70 - 49\,\frac{t}{t_f} \\ \delta\gamma_Q &= 2\,\frac{\pi}{180} \\ \delta\psi_Q &= \frac{\pi}{180}\left(7 - 6\,\frac{t}{t_f}\right) \end{aligned}\right\} \qquad (30)$$

$$\left.\begin{aligned} \delta\alpha_R &= 3 + 12\,\frac{t}{t_f} \\ \delta\phi_R &= \frac{1.7\pi}{180}\left(1 + \frac{t}{t_f}\right) \\ \delta\left(\frac{T}{m}\right)_R &= 0.17 + 0.1\prime\,\frac{t}{t_f} \end{aligned}\right\} \qquad (31)$$

$$\left.\begin{aligned} \delta x_M &= 55 & \delta V_M &= 21 \\ \delta y_M &= 9 & \delta\gamma_M &= 2\,\frac{\pi}{180} \\ \delta z_M &= 5 & \delta\psi_M &= \frac{\pi}{180} \end{aligned}\right\} \qquad (32)$$

These weights were arrived at experimentally by using the iterative process described above.

There are several constraints imposed upon the design. To avoid passenger discomfort, angular rates should not exceed 10° per sec and by federal regulation, roll angle cannot exceed 30°. Engine thrust can be throttled between 12.45 and 124.5 kN (2800 and 28 000 lb) which correspond to thrust-mass ratios of 0.3 and 3 m/sec^2. Final errors in the states will be a function of how well the weighting matrices are chosen, the magnitude of the initial state errors, wind velocity and direction, and of the particular flight path chosen. After the wings-level maneuver the aircraft is headed north at about 62 m/sec, and since the runways are normally much longer than necessary for this aircraft, an error in x of ± 62 m (i.e., approximately 1 sec) is not unreasonable. However, errors in y of greater than ± 10 m are unacceptable. The fact that the runway is normally only 50 m wide and the wing span is approximately 30 m makes an error of 10 m undesirable even though some correction will be made during flare. Errors in velocity V and flight-path angle γ are best viewed in terms of sink rate $\dot{z}$ ($\dot{z} = V \sin \gamma$). This error should be kept within ± 1.0 m/sec while a negative error (slower descent) is preferred. Error in heading should be kept within 5°. An error of that size can be nulled by a decrab maneuver. The most troublesome errors in this study turned out to be in y during the 6° approaches.

Representative Landing Approach

Time histories from a representative flight are shown in figure 4. The nominal curves are shown as dotted lines and the simulated flight (path 2A) as a continuous curve. This was a 6° approach with nominal initial heading due east and initial altitude of 550 m. The six states and three controls are shown, along with an overview of the XY-plane. The aircraft started wings level with a heading of 80° (10° error). It was 100 m higher than nominal and had more than a 300-m error in both x and y. The velocity was low by about 20 percent. The aircraft was near stall, and consequently, the angle of attack and throttle setting were set high for trim. These errors which are extreme were chosen to demonstrate the control-system performance. The plane was subjected to a 15-knot constant east wind. Immediately, the aircraft rolled with some overshoot to the 23° nominal bank angle. The angle of attack was decreased and the throttle was cut back. This made the aircraft simultaneously pitch over and increase speed while initiating its curved descending turn to the right. The rollout at a 100-m altitude is apparent in the curves of y, ψ, and ϕ. The entire approach lasted about 82 sec and rollout occurred at around 70 sec. The simulation was terminated when the plane reached an altitude of around 15 m just above where the flare would be executed. Most of the motion is smooth but roll-angle rate definitely reaches its 10°/sec limit and the thrust-mass ratio stays on its lower limit of 0.3 (T = 12.5 kN (2800 lb)) for much of the run. The overshoot in roll angle (-10°) at rollout is undesirable, but is much less apparent in the 3° approaches. It could, most likely, be considerably reduced by making the nominal roll angle a contin-

uous function. However, this would complicate (perhaps unjustifiably) the entire control system. At decision height, the aircraft was within 1 sec of the nominal. Final errors for this flight were -71 m, 0.0 m, -0.1 m, 3.9 m/sec, -0.8°, 0.1°, and -0.6 m/sec for x, y, z, V, γ, ψ, and $\dot{z}$, respectively.

Representative Feedback Gains

The elements of the feedback gain matrix K for flight path 2A are shown in figure 5. The magnitude of the gains, in general, increase with time due to the time variation of the weighting matrices Q and R. Some of the gains have a pronounced increase in the last several seconds of flight due to the influence of the M matrix. (See figs. 5(c), (g), and (k).) During the straight-in portion of the approach, 10 of the 18 gains are zero or can be considered zero. Of course, the more of these elements that are zero or near zero, the easier it is to implement the control system. In order to determine the influence of a particular gain, one assumes a large reasonable error in the state and then calculates the resulting change in the control. If the change is insignificant, then the element can be considered zero. For example, an error of 3 m in z near the end of the flight would only change the thrust-mass ratio by 0.06. Whereas an error in x of 60 m would cause the ratio to change by 1.2. Since these are both large reasonable errors at the termination of flight, the element K_{33} should be considered zero. Using this approach, it can be seen that after rollout, thrust-mass ratio is a function only of x and V, roll angle is a function of only y and ψ, and angle of attack is a function of x, V, z, and γ. This partial decoupling is useful to the designer in the iterative process of choosing the weighting matrices. Applying the same reasoning, five elements of K can be considered zero throughout the entire flight. They are K_{23}, K_{24}, K_{25}, K_{35}, and K_{36}. Each of the time histories of the remaining 13 gains would have to be stored in the on-board computer. Eleven points with linear interpolation could easily approximate any of these functions. Some of them could be fitted by low order polynomials in time which would require even less parameter storage. It appears that the entire gain matrix and nominal path could be stored in less than 200 words of storage. This number could probably be reduced but it is important to realize that any parameter change in the nominal-state trajectory will affect these gains. Each airport using this system would probably have several different nominal approaches and these would also probably differ among airports. To be practical then, the computer must have access to the correct set of parameters out of many possible alternative sets. Several possible ways of accomplishing this are

(1) All necessary parameter sets are stored in an on-board mass storage device.

(2) The particular set of parameters needed is calculated on the airborne computer prior to landing approach.

(3) The parameter set is transmitted from the airport to the on-board computer when the landing approach is assigned.

(4) The feedback gains could possibly be expressed as analytic functions of time and the five primary parameters of the nominal flight path.

The feedback gains of figure 5 were calculated using the weighting matrices M, Q, and R as given in equations (30) to (32). The gains were used in the landing approach shown in figure 4. This choice of weighting matrices and resulting gains appears adequate for this flight path and control task.

System Performance

The control system was tested on each of the seven landing approaches described in table 2. Results from the first six flight paths are given in tables 3 to 8 and from flight path 3B in table 9. Each of these seven tables represent 25 simulated landing approaches. On each approach, the aircraft was subjected to a constant wind of 15 knots magnitude from a direction ψ_W. The direction changed for each approach and it was generated as a random variable with uniform distribution between -180^o and $+180^o$. Each approach was started with off-nominal errors in all state variables. These initial errors were generated as random variables. They were normally (Gaussian) distributed with zero mean. The standard deviations selected for the six state errors in x, y, z, V, γ, and ψ, respectively, were 100 m, 100 m, 30 m, 3 m/sec, 1^o, and 3^o. Each flight path had a distinct random sequence of sets of initial state errors.

The reason for employing randomness in the control task was that the system showed that it could be tuned to a particular task. Originally, only 90^o crosswinds were used because they were thought to be a worse case. Then it was discovered that winds from the aft quarter occasionally gave more trouble. Because this aircraft has a high lift-to-drag ratio, these winds were particularly difficult on the steep approaches. Also, certain combinations of initial errors were easier to correct than others. Therefore, a strong wind randomly directed was used and the aircraft was initialized with large random off-nominal errors. The controls were initially set such that the wings were level ($\phi = 0$) and the aircraft was trimmed.

Table 3 presents the data for the 25 landing approaches along flight path 1. The mean, standard deviation, and range of initial errors are given for each state. The measured statistics of the initial state errors differ from their ideal values because they represent a subset of a very long pseudo random sequence which has the selected statistics. The initial off-nominal values of the controls are not really errors, but show a variation in initial trim values. Roll angle is a constant -12.2^o since the approach always starts wings level rather than rolled over at 12.2^o. The final off-nominal errors taken just above the flare altitude show how well the control system did its work. Statistics

are given on the six state variables and sink rate $\dot{z}$. As can be seen, the control system worked very well on flight path 1. Poor performance usually makes itself apparent in final errors in y and z. For these 25 runs, the approaching aircraft was never more than 1 m from the centerline of the runway and the final error in altitude was never greater than 1.1 m. Since the nominal sink rate is 3.24 m/sec, the maximum error in final altitude corresponds to about one-third of a second in time. This same observation can be made with regard to x since nominal $\dot{x}$ is approximately 62 m/sec and the maximum final error in x for the 25 runs was 24.7 m. Table 3 also indicates how much control was needed to fly the aircraft. For each of the 25 approaches, the largest off-nominal control excursion is identified whether it be positive or negative. The initial transient of each run was not included since the initial off-nominal values of at least roll angle would always be extreme for the flight and it would mask the desired information. So, for example, the average extreme for angle of attack was 4.6° greater than the nominal and the extreme varied over the 25 flights from 3.3° to 5.7° above nominal. The table also gives information on extreme control rates for each run. These are important mainly in how they affect passenger comfort. The statistics given are on the extremes of each flight including the initial transient. Finally, the table gives the number of flights which were unacceptable because one or more of the constraints, discussed in the section on design consideration, was violated.

As can be seen from examining tables 3, 4, and 5, the control system was quite effective on flight paths 1, 2, and 3, respectively. The largest final errors for these 75 approaches were 2.1 m in y and 1.2 m in z. There were no unacceptable flights; both control excursion and control rates were moderate.

Tables 6 to 8 show the results for the 6° approaches. As can be seen, the control system did not do as well on these approaches. Final errors in y and ψ were larger, and roll angle tended to have larger off-nominal excursions.

On path 1A, the mean final error in y was a disturbing 9.3 m. Because the aircraft did not execute the wings-level maneuver fast enough, it tended to go off to the right (east), and then it would roll to the left in order to get back on the centerline. On these 6° approaches, there were only about 13 sec from initiation of rollout to the conclusion of the simulation. Since the variation of the error is small (1.3), performance on this flight path could probably be improved by starting the rollout a few seconds early. This is, in fact, what pilots have been observed to do when flying this approach. On flight path 2A, performance is slightly worse and nine of these had final errors in y which were greater than 10 m and consequently were unacceptable. The variation in final y-error was again small, indicating that a slight adjustment in the flight path could possibly bring the errors within ±4.4 m. Finally, on flight path 3A, the control system proved to be completely inadequate with 18 of the 25 flights having final errors in y which were greater than 10 m. It is possible that another choice of weights, specifically δy_Q and

δy_M, might improve performance on the 6° flight paths. However, the principal problem seems to be one of time. Flight time decreases monotonically from 212 sec on flight path 1 to around 60 sec on flight path 3A. It appears that the 6° approaches do not have enough time to null out initial errors and the adverse effect of crosswinds. In order to support this premise, flight path 3A was modified such that initial altitude was 500 m instead of 400 m, and rollout was accomplished at 200 m instead of 100 m. This new flight path is labeled 3B. Its parameters are given in table 2 and its performance is reported in table 9. In order to facilitate comparison of table 9 and table 8, the exact same sequences of initial errors and wind directions were used. The flight time for 3B was about 15 sec longer than 3A, and all of this was added to the straight-in portion of the flight. The marked improvement in performance of 3B over 3A is apparent when table 9 is compared with table 8. On 3B, 8 approaches exceeded the allowable limit of a 10-m final error in y; whereas on 3A, 18 approaches exceeded it. Since this improvement seems to be caused by the increased flying time, it may follow that doubling the initial nominal altitude and rollout altitude on the 6° approaches would lead to performance comparable to that experienced on the 3° approaches.

Finally, the control system was tested for sensitivity to uncertainties in the aerodynamics of the aircraft and for normal variation in the atmosphere. A particular landing approach was used. Initial errors and wind direction were not varied. Twenty-five simulation runs were made, each with a different atmospheric density function and each with a different set of values for the aerodynamic parameters in table 1. The results of these flights are given in table 10. All six aircraft parameters were allowed to vary randomly from run to run. The values given in table 1 were used as the mean and 4 percent of those values were used as the standard deviation. The distribution was normal. This resulted in a random variation in these parameters of about ±10 percent. Air density, as described in equation (7), was also given random variation. The multiplying coefficient 1.22 of that equation was allowed to vary normally with mean 1.22 and standard deviation of 0.0244. This resulted in a random variation of air density of about ±5 percent for any particular altitude. These variations seemed only to propagate into the final errors in x, z, and V and into the extreme control excursions in angle of attack. None of these final errors were large enough to cause concern. The control system appears to handle these normal variations and uncertainties quite well.

CONCLUDING REMARKS

Linear optimal regulator theory is applied to a nonlinear simulation of an aircraft performing a helical landing approach. The nonlinear equations of motion are developed and are linearized (time-varying coefficients) about a quasi-steady helical flight path. The nominal-state time histories are given as explicit functions of time and a numerical

method for determining the constant-control inputs is presented. Control of the system to the nominal-state trajectories is posed as a regulator problem with time-varying weighting matrices in the cost functional. A method of solving for the feedback gain matrix is reviewed.

The theory was then implemented in a simulation of a small two-engined transport airplane, and system performance was measured for seven distinct approaches including flight path angles (descent angles) of 3° and 6°. On each approach, the aircraft was subjected to large errors in initial values of state variables and to strong steady crosswinds. The system was also tested for sensitivity to normal variations in atmosphere and to reasonable uncertainties in the parametric description of the aircraft. Statistical data on 200 simulated landings are presented.

The control system performed very well on all the 3° approaches and was reasonably insensitive to changes in the atmosphere and to parametric changes in the aircraft model. Performance, which was measured in terms of terminal errors, violation of design constraints, and passenger comfort, was not nearly as good on the 6° approaches. These approaches are more difficult to execute since descent rate and roll angle are doubled, radius of the helix is halved, and flight time is halved. On the most difficult of these 6° approaches, the total flight time was about 60 sec, and performance was definitely unacceptable. Evidence is presented to support the contention that total flight time is the critical factor and that performance on the 6° paths could be greatly improved by starting the approach from a higher altitude which would result in a larger turning radius and longer flight times. This hypothesis needs to be tested further if 6° approaches are a requirement.

The control-system design method used in this study is relatively straight forward and is easy to implement with the aid of a modern computer. The only difficulty is in choosing the weighting matrices for the cost functional. It was concluded that the weights should be time varying for the particular control task studied. This method should be extended to the more complex simulation, which includes both actuators and sensors and has six-degree-of-freedom dynamics, before being implemented on the aircraft.

Langley Research Center
National Aeronautics and Space Administration
Hampton, Va. 23665
June 9, 1975

APPENDIX

JACOBIAN MATRICES USED IN THE LINEARIZATION OF THE AIRCRAFT DYNAMICS

The aircraft dynamics were linearized about a nominal-state trajectory and nominal-control time history. This was done in order to apply linear optimal regulator theory to the computation of the feedback gains. As is evident in equation (3) of the text, the Jacobian matrices

$$A(t) = \frac{\partial \bar{f}}{\partial \bar{x}} \qquad B(t) = \frac{\partial \bar{f}}{\partial \bar{u}}$$

are needed. These are

$$\frac{\partial \bar{f}}{\partial \bar{u}} = \begin{bmatrix} 0 & 0 & 0 \\ 0 & 0 & 0 \\ 0 & 0 & 0 \\ -\left(\frac{\partial D/\partial \alpha}{m} + \frac{T}{m} \sin \alpha\right) & 0 & \cos \alpha \\ -\left(T \cos \alpha + \frac{\partial L}{\partial \alpha}\right) \cos \phi & (L + T \sin \alpha) \sin \phi & -\sin \alpha \cos \phi \\ \hline mV & mV & V \\ \left(\frac{\partial L}{\partial \alpha} + T \cos \alpha\right) \sin \phi & (L + T \sin \alpha) \cos \phi & \sin \alpha \sin \phi \\ \hline mV \cos \gamma & mV \cos \gamma & V \cos \gamma \end{bmatrix} \tag{A1}$$

where

$$\frac{\partial L}{\partial \alpha} = qSC_{L_\alpha} \frac{\pi}{180}$$

$$\frac{\partial D}{\partial \alpha} = 2qSC_{L_\alpha}^2 \eta \left(\frac{\pi}{180}\right)^2 (\alpha - \alpha_o)$$

and

$$\frac{\partial \bar{f}}{\partial \bar{x}} = \begin{bmatrix} 0 & 0 & 0 & \cos\gamma\cos\psi & -V\sin\gamma\cos\psi & -V\cos\gamma\sin\psi \\ 0 & 0 & 0 & \cos\gamma\sin\psi & -V\sin\gamma\sin\psi & V\cos\gamma\cos\psi \\ 0 & 0 & 0 & \sin\gamma & V\cos\gamma & 0 \\ 0 & 0 & 0 & \frac{-2D}{mV} & g\cos\gamma & 0 \\ 0 & 0 & 0 & \left(\frac{T}{m}\sin\alpha\cos\phi - g\cos\gamma - \frac{L}{m}\cos\phi\right)V^{-2} & \frac{g}{V}\sin\gamma & 0 \\ 0 & 0 & 0 & \frac{(L + T\sin\alpha)\sin\phi}{mV^2\cos\gamma} & \frac{(L + T\sin\alpha)\sin\phi\sin\gamma}{mV\cos^2\gamma} & 0 \end{bmatrix} \quad \text{(A2)}$$

An assumption that atmospheric density is constant over the range of altitude considered is incorporated into these equations. This assumption is discussed in the text. It is not made in the nonlinear simulation which uses the feedback gains.

REFERENCES

1. Reeder, John P.; Taylor, Robert T.; and Walsh, Thomas M.: New Design and Operating Techniques for Improved Terminal Area Compatability. [Preprint] No. 740454, Soc. Automot. Eng., Apr.-May 1974.

2. Athans, Michael; and Falb, Peter L.: Optimal Control. McGraw-Hill Book Co., Inc., c.1966.

3. Bryson, Arthur E., Jr.; and Ho, Yu-Chi: Applied Optimal Control. Blaisdell Pub. Co., c.1969.

4. Kwakernaak, Huibert; and Sivan, Raphael: Linear Optimal Control Systems. John Wiley & Sons, Inc., c.1972.

5. Hsu, Jay C.; and Meyer, Andrew U.: Modern Control Principles and Applications. McGraw-Hill Book Co., Inc., c.1968.

6. Meditch, J. S.: Stochastic Optimal Linear Estimation and Control. McGraw-Hill Book Co., c.1969.

7. Hoffman, William C.; Zvara, John; and Bryson, Arthur E.: A Landing Approach Guidance Scheme for Unpowered Lifting Vehicles. J. Spacecraft & Rockets, vol. 7, no. 2, Feb. 1970, pp. 196-202.

8. Burrows, James W.; and Tobie, H. N.: Linear Energy Management During Unpowered Landing Approach. Doc. No. D6-24909TN, Boeing Co., [1971].

9. Olason, M. L.; and Norton, D. A.: Aerodynamic Design Philosophy of the Boeing 737. J. Aircraft, vol. 3, no. 6, Nov.-Dec. 1966, pp. 524-528.

10. Harrison, Neil: Boeing 737 – A Short-Hauler Engineered for Efficiency. Flight Int., vol. 89, no. 2969, Feb. 3, 1966, pp. 181-188.

11. U.S. Standard Atmosphere Supplements, 1966. Environ. Sci. Serv. Admin., NASA, and U.S. Air Force, 1966.

12. Scarborough, James B.: Numerical Mathematical Analysis. Fourth ed. Johns Hopkins Press, 1958.

13. Kalman, R. E.; and Englar, T. S.: A User's Manual for the Automatic Synthesis Program (Program C). NASA CR-475, 1966.

TABLE 1.- PARAMETERS OF THE AIRPLANE

(GEAR DOWN, FLAPS AT 40°)

Lift-curve slope C_{L_α}, rad^{-1}	7.162
Angle of attack for zero lift α_o, deg	-10.4
Drag coefficient for zero lift $C_{D,o}$	0.157
Efficiency factor η	0.0314
Aeodynamic reference area S, m^2	91.04
Mass of vehicle m, κg	40 823

TABLE 2.- PARAMETRIC DESCRIPTION OF NOMINAL FLIGHT PATHS

[V = 62 m/sec]

Flight path	Initial altitude h_0, m	Rollout altitude $-z_{SI}$, m	Descent angle γ, deg	Initial heading ψ_0, deg	Sink rate $\dot{z}$, m/sec	Radius of helix, m	Roll angle ϕ, deg	Turn rate $\dot{\psi}$, deg/sec	Rollout time t_{SI}, sec	Final time t_f, sec
1	700	100	3	0	3.24	1822	12.2	1.95	185.0	215.5
2	550	100	3	90	3.24	1822	12.2	1.95	138.5	169.5
3	400	100	3	180	3.24	1822	12.2	1.95	92.5	123.0
1A	700	100	6	0	6.48	909	23.3	3.89	93.0	108.0
2A	550	100	6	90	6.48	909	23.3	3.89	69.5	85.0
3A	400	100	6	180	6.48	909	23.3	3.89	46.5	61.5
3B	500	200	6	180	6.48	909	23.3	3.89	46.5	77.0

TABLE 3.- STATISTICAL DATA FROM 25 LANDING APPROACHES ALONG FLIGHT PATH 1

$[\gamma = 3^{o}$; $\dot{z} = 3.24$ m/sec; $V_W = 15$ knots; $\psi_W = U(-180^{o}, 180^{o})$; $t_f = 211.5$ sec; $h_f = 13.7$ m; $x_f = -262$ m$]$

Variable	Mean	Standard deviation	Range
	Initial off-nominal errors		
x, m	-6.9	64.7	-146 to 119
y, m	-13.0	84.5	-153 to 193
z, m	-4.1	32.1	-85 to 76
V, m/sec	.6	2.8	-4.2 to 5.2
γ, deg	.2	.8	-1.3 to 1.9
ψ, deg	.5	3.1	-6.1 to 8.6
α, deg	.1	1.4	-2.1 to 2.7
ϕ, deg	-12.2	0	
T/m, m/sec^2	-.05	.14	-.36 to .20
	Final off-nominal errors (at decision altitude)		
x, m	-10.2	9.5	-24.7 to -0.0
y, m	.6	.3	.4 to 1.0
z, m	.0	.6	-.6 to 1.1
V, m/sec	.2	.4	-.3 to .7
γ, deg	.0	.2	-.3 to .4
ψ, deg	-.2	.1	-.3 to -.1
$\dot{z}$, m/sec	.03	.25	-.28 to .40
	Extreme off-nominal excursions during each flight		
α, deg	4.6	0.5	3.3 to 5.7
ϕ, deg	-.4	2.2	-2.3 to 3.9
T/m, m/sec^2	.09	.22	-.40 to .40
	Extreme control rate during each flight		
$\dot{\alpha}$, deg/sec	0.3	1.5	-2.5 to 3.3
$\dot{\phi}$, deg/sec	7.8	3.1	-6.7 to 9.4
$\dot{T}$/m, m/sec^3	-.03	.15	-.23 to .25
Number of unacceptable flights = 0			

TABLE 4.- STATISTICAL DATA FROM 25 LANDING APPROACHES ALONG FLIGHT PATH 2

[$\gamma = 3^o$; $\dot{z} = 3.24$ m/sec; $V_w = 15$ knots; $\psi_w = U(-180^o, 180^o)$; $t_f = 165$ sec; $h_f = 14.6$ m; $x_f = -279$ m]

Variable	Mean	Standard deviation	Range
	Initial off-nominal errors		
x, m	8.4	118.1	-292 to 236
y, m	10.5	93.9	-199 to 179
$\dot{z}$, m	2.3	21.5	-27 to 48
V, m/sec	.2	2.7	-4.8 to 6.9
γ, deg	.2	.9	-1.4 to 2.9
ψ, deg	-.9	2.2	-5.7 to 3.0
α, deg	.1	1.3	-2.9 to 2.8
ϕ, deg	-12.1	0	
T/m, m/sec^2	-.06	.14	-.46 to .19
	Final off-nominal errors (at decision altitude)		
x, m	-9.4	8.1	-26.3 to 0.4
y, m	.8	.4	.3 to 1.3
z, m	-.1	.6	-.7 to 1.2
V, m/sec	.1	.3	-.3 to .8
γ, deg	-.0	.2	-.3 to .4
ψ, deg	-.2	.1	-.3 to -.1
$\dot{z}$, m/sec	-.01	.23	-.33 to .41
	Extreme off-nominal excursions during each flight		
α, deg	2.9	3.2	-3.7 to 6.5
ϕ, deg	4.1	.1	4.0 to 4.3
T/m, m/sec^2	.08	.19	-.34 to .39
	Extreme control rate during each flight		
$\dot{\alpha}$, deg/sec	0.5	1.9	-3.0 to 4.8
$\dot{\phi}$, deg/sec	8.8	.7	6.7 to 9.4
$\dot{T}$/m, m/sec^3	-.0	.15	-.29 to .23
	Number of unacceptable flights = 0		

TABLE 5.- STATISTICAL DATA FROM 25 LANDING APPROACHES ALONG FLIGHT PATH 3

[$\gamma = 3^o$; $\dot{z} = 3.24$ m/sec; $V_w = 15$ knots; $\psi_w = U(-180^o, 180^o)$; $t_f = 118.5$ sec; $h_f = 15.5$ m; $x_f = -296$ m]

Variable	Mean	Standard deviation	Range
	Initial off-nominal errors		
x, m	11.1	95.2	-176 to 174
y, m	-12.8	104.1	-209 to 217
z, m	-2.5	30.8	-48 to 73
V, m/sec	-.0	2.1	-3.7 to 5.2
γ, deg	-.1	1.1	-1.8 to 1.8
ψ, deg	.4	2.5	-4.1 to 6.2
α, deg	-.1	1.0	-2.4 to 1.8
ϕ, deg	-12.1	0	
T/m, m/sec^2	-.02	..20	-.35 to .29
	Final off-nominal errors (at decision altitude)		
x, m	-9.4	10.5	-29.1 to 3.4
y, m	.8	.6	-.3 to 2.1
z, m	.1	.5	-.5 to 1.0
V, m/sec	.1	.6	-.7 to 1.2
γ, deg	.1	.3	-.3 to .6
ψ, deg	-.2	.1	-.5 to -.1
$\dot{z}$, m/sec	.09	.21	-.31 to .72
	Extreme off-nominal excursions during each flight		
α, deg	2.8	3.1	-3.8 to 7.0
ϕ, deg	7.1	.2	6.8 to 7.4
T/m, m/sec^2	.08	.23	-.18 to .49
	Extreme control rate during each flight		
$\dot{\alpha}$, deg/sec	-0.2	1.8	-3.5 to 2.6
$\dot{\phi}$, deg/sec	8.3	.9	6.1 to 9.4
$\dot{T}$/m, m/sec^3	-.00	.13	-.24 to .19
Number of unacceptable flights = 0			

TABLE 6.- STATISTICAL DATA FROM 25 LANDING APPROACHES ALONG FLIGHT PATH 1A

[$\gamma = 6^o$; $\dot{z} = 6.28$ m/sec; $V_w = 15$ knots; $\psi_w = U(-180^o, 180^o)$; $t_f = 105.5$ sec; $h_f = 19.5$ m; $x_f = -186$ m]

Variable	Mean	Standard deviation	Range
		Initial off-nominal errors	
x, m	27.4	112.7	-219 to 276
y, m	13.3	106.0	-224 to 237
z, m	-7.7	26.7	-60 to 40
V, m/sec	-.1	3.6	-7.2 to 6.4
γ, deg	.1	1.1	-1.5 to 2.4
ψ, deg	-.3	3.3	-6.8 to 6.3
α, deg	-.4	1.9	-3.4 to 3.7
ϕ, deg	-23.2	0	
T/m, m/sec^2	-.07	.11	-.17 to .17
		Final off-nominal errors (at decision altitude)	
x, m	-11.3	11.3	-29.3 to 12.1
y, m	9.3	1.3	6.6 to 11.6
z, m	-.5	.6	-1.1 to .8
V, m/sec	.1	.6	-1.4 to 1.1
γ, deg	.1	.2	-.3 to .4
ψ, deg	-2.0	.3	-2.5 to -1.4
$\dot{z}$, m/sec	.14	.32	-.47 to .62
		Extreme off-nominal excursions during each flight	
α, deg	3.2	3.8	-3.7 to 8.4
ϕ, deg	19.1	.2	18.8 to 19.4
T/m, m/sec^2	.19	.18	-.17 to .47
		Extreme control rate during each flight	
$\dot{\alpha}$, deg/sec	0.4	2.1	-3.3 to 4.1
$\dot{\phi}$, deg/sec	-10.0	0	
$\dot{T}$/m, m/sec^3	.00	.11	-.21 to .22
		Number of unacceptable flights = 9	

TABLE 7.- STATISTICAL DATA FROM 25 LANDING APPROACHES ALONG FLIGHT PATH 2A

[$\gamma = 6^o$; $\dot{z} = 6.28$ m/sec; $V_w = 15$ knots; $\psi_w = U(-180^o, 180^o)$; $t_f = 82.5$ sec; $h_f = 15.3$ m; $x_f = -146$ m]

Variable	Mean	Standard deviation	Range
	Initial off-nominal errors		
x, m	-9.7	89.2	-235 to 147
y, m	20.8	75.4	-143 to 192
z, m	1.2	26.2	-41 to 56
V, m/sec	.3	3.4	-6.9 to 6.2
γ, deg	-.0	.8	-2.1 to 1.4
ψ, deg	-.3	2.5	-3.5 to 6.9
α, deg	-.9	1.7	-3.6 to 3.2
ϕ, deg	-23.2	0	
T/m, m/sec^2	-.07	.11	-.17 to .24
	Final off-nominal errors (at decision altitude)		
x, m	-2.9	10.3	-29.4 to 15.8
y, m	9.4	2.6	5.3 to 14.0
z, m	-.4	1.0	-1.9 to 1.3
V, m/sec	-.5	.6	-1.5 to 1.1
γ, deg	.1	.3	-.4 to .4
ψ, deg	-1.8	.5	-2.8 to -1.0
$\dot{z}$, m/sec	.02	.24	-.35 to .32
	Extreme off-nominal excursions during each flight		
α, deg	3.3	3.1	-4.2 to 6.3
ϕ, deg	13.2	.3	12.8 to 14.0
T/m, m/sec^2	.08	.16	-.17 to .31
	Extreme control rate during each flight		
$\dot{\alpha}$, deg/sec	-0.1	2.0	-3.4 to 3.8
$\dot{\phi}$, deg/sec	-10.0	0	
$\dot{T}$/m, m/sec^3	-.03	.11	-.17 to .21
Number of unacceptable flights = 9			

TABLE 8.- STATISTICAL DATA FROM 25 LANDING APPROACHES ALONG FLIGHT PATH 3A

[$\gamma = 6^o$; $\dot{z} = 6.28$ m/sec; $V_W = 15$ knots; $\psi_W = U(-180^o, 180^o)$; $t_f = 59.0$ sec; $h_f = 15$ m; $x_f = -140$ m]

Variable	Mean	Standard deviation	Range
	Initial off-nominal errors		
x, m	-35.6	88.4	-225 to 129
y, m	-22.2	89.5	-266 to 81
z, m	-5.2	36.3	-61 to 54
V, m/sec	.1	2.5	-6.0 to 4.2
γ, deg	.1	.9	-1.3 to 2.3
ψ, deg	-.3	2.8	-5.4 to 4.7
α, deg	-1.1	1.3	-3.0 to 2.4
ϕ, deg	-23.2	0	
T/m, m/sec^2	-.07	.09	-.17 to .09
	Final off-nominal errors (at decision altitude)		
x, m	-21.7	17.9	-57.4 to 11.4
y, m	13.2	8.5	-12.4 to 26.4
z, m	-.5	.7	-2.0 to 1.2
V, m/sec	1.1	1.1	-1.1 to 2.9
γ, deg	.1	.2	-.4 to .3
ψ, deg	-2.5	1.7	-5.2 to 2.6
$\dot{z}$, m/sec	.18	.28	-.34 to .63
	Extreme off-nominal excursions during each flight		
α, deg	0.5	4.2	-4.2 to 7.2
ϕ, deg	21.4	.8	19.6 to 22.8
T/m, m/sec^2	.23	.20	-.17 to .62
	Extreme control rate during each flight		
$\dot{\alpha}$, deg/sec	1.1	1.8	-2.0 to 5.1
$\dot{\phi}$, deg/sec	-10.0	0	
$\dot{T}$/m, m/sec^3	.03	.10	-.15 to .15
Number of unacceptable flights = 18			

TABLE 9.- STATISTICAL DATA FROM 25 LANDING APPROACHES ALONG FLIGHT PATH 3B

[$\gamma = 6^o$; $\dot{z} = 6.28$ m/sec; $V_W = 15$ knots; $\psi_W = U(-180^o, 180^o)$; $t_f = 75.0$ sec; $h_f = 14.7$ m; $x_f = -135$ m]

Variable	Mean	Standard deviation	Range
	Initial off-nominal errors		
x, m	-35.6	88.4	-225 to 129
y, m	-22.2	89.5	-266 to 81
z, m	-5.2	36.3	-61 to 54
V, m/sec	.1	2.5	-6.0 to 4.2
γ, deg	.1	.9	-1.3 to 2.3
ψ, deg	-.3	2.8	-5.4 to 4.7
α, deg	-.9	1.3	-2.9 to 2.6
ϕ, deg	-23.2	0	
T/m, m/sec^2	-.07	.09	-.17 to .09
	Final off-nominal errors (at decision altitude)		
x, m	-17.1	16.5	-48.4 to 18.8
y, m	7.7	4.0	-3.1 to 14.2
z, m	-.6	.6	-1.5 to .7
V, m/sec	.8	.8	-.6 to 2.4
γ, deg	.1	.2	-.7 to .4
ψ, deg	-1.2	.6	-2.2 to .5
$\dot{z}$, m/sec	.14	.3	-.64 to .60
	Extreme off-nominal excursions during each flight		
α, deg	0.9	4.1	-4.0 to 7.1
ϕ, deg	21.3	.7	19.4 to 22.6
T/m, m/sec^2	.21	.19	-.17 to .55
	Extreme control rate during each flight		
$\dot{\alpha}$, deg/sec	1.0	1.8	-2.0 to 5.0
$\dot{\phi}$, deg/sec	-10.0	0	
$\dot{T}$/m, m/sec^3	.0	.1	-.15 to .16
Number of unacceptable flights = 8			

TABLE 10.- STATISTICAL DATA FROM 25 LANDING APPROACHES ALONG FLIGHT PATH 2 WITH VARIATIONS IN THE AERODYNAMIC PARAMETERS. RANDOM VARIATION OF APPROXIMATELY ±10 PERCENT IN AIRCRAFT PARAMETERS AND ±5 PERCENT IN AIR DENSITY

$[\gamma = 3^{o}$; $\dot{z} = 3.24$ m/sec; $V_W = 15$ knots; $\psi_W = 170^{o}$; $t_f = 165$; $h_f = 14.6$ m; $x_f = -279$ m$]$

Variable	Mean	Standard deviation	Range
		Initial off-nominal errors	
x, m	186.0		
y, m	157.9		
z, m	-24.0		
V, m/sec	1.4		
γ, deg	-.2		
ψ, deg	2.1		
α, deg	-.6		
ϕ, deg	-12.1		
T/m, m/sec^2	.01		
		Final off-nominal errors (at decision altitude)	
x, m	1.7	3.7	-4.3 to 12.2
y, m	.4	.1	.3 to .5
z, m	1.0	.4	.0 to 1.6
V, m/sec	-.3	.2	-.8 to -.1
γ, deg	.4	.0	.3 to .4
ψ, deg	-.1	.0	-.1 to -.1
$\dot{z}$, m/sec	.37	.05	.27 to .46
		Extreme off-nominal excursions during each flight	
α, deg	3.2	2.6	-3.8 to 5.1
ϕ, deg	4.1	.0	4.1 to 4.2
T/m, m/sec^2	-.20	.03	-.34 to -.29
		Extreme control rate during each flight	
$\dot{\alpha}$, deg/sec	-1.0	0.1	-1.2 to -0.8
$\dot{\phi}$, deg/sec	8.9	.0	8.9 to 8.9
$\dot{T}$/m, m/sec^3	-.18	.00	-.19 to -.18
		Number of unacceptable flights = 0	

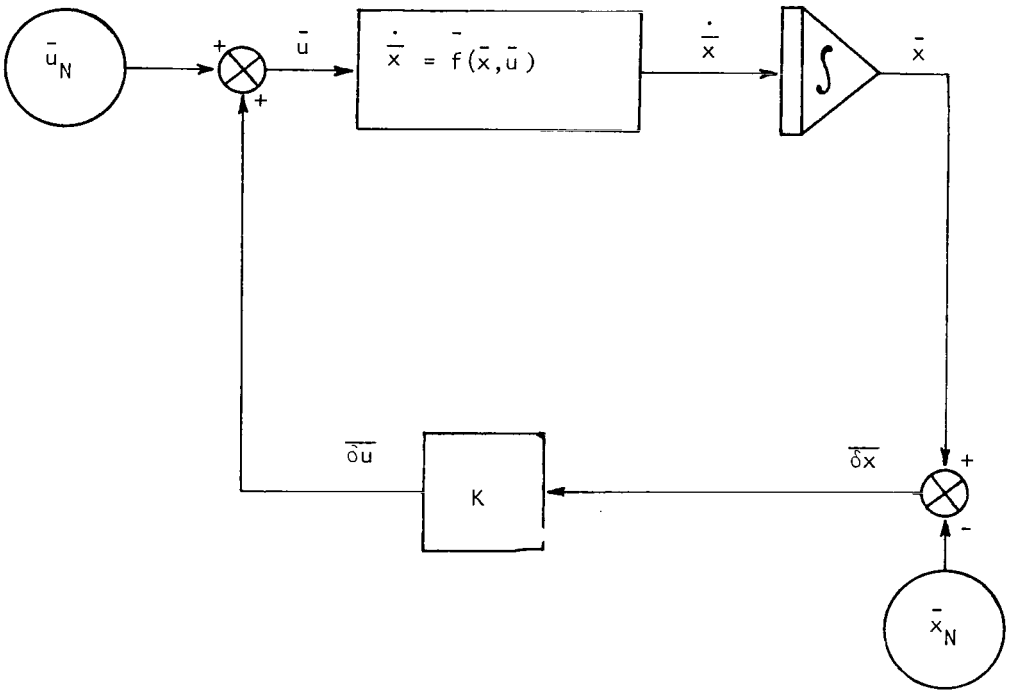

Figure 1.- Schematic diagram of aircraft landing simulation.

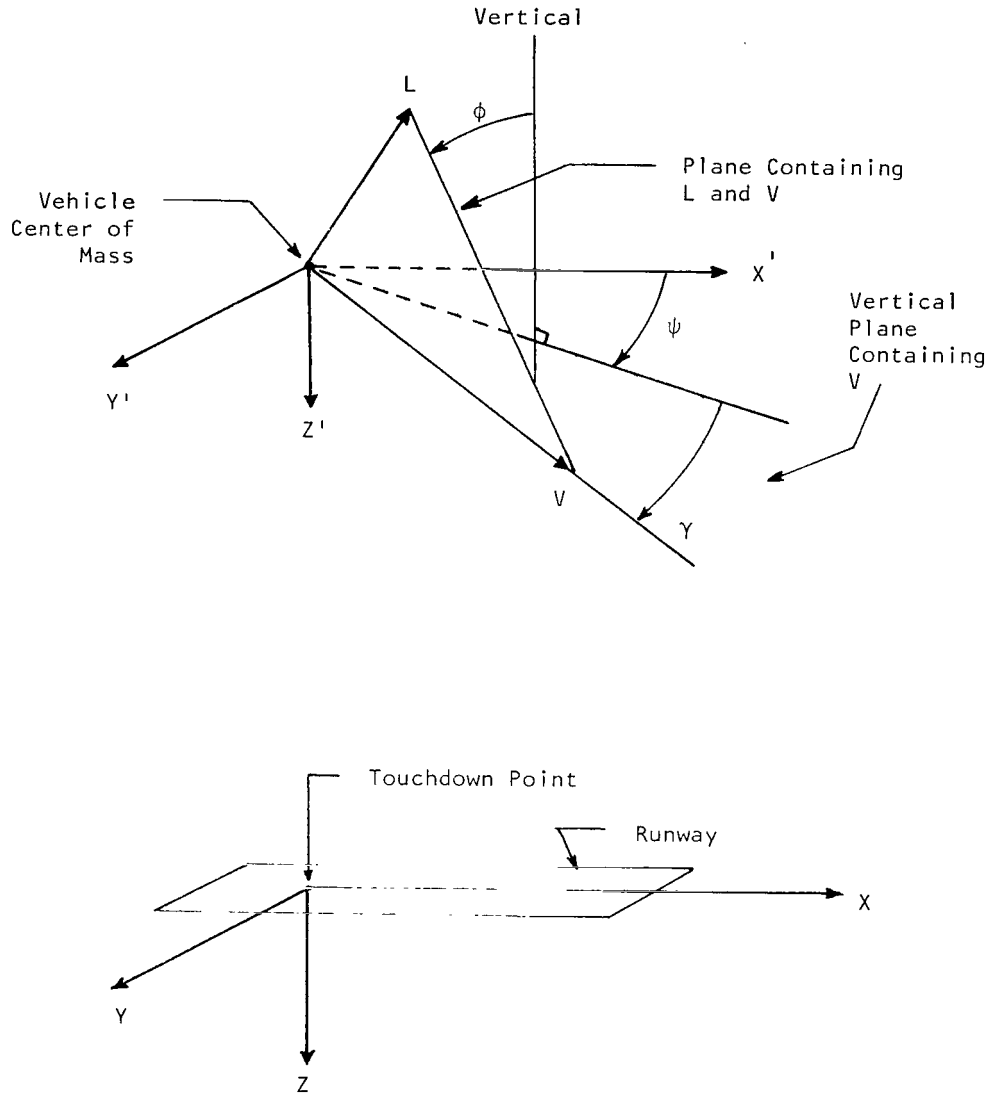

Figure 2.- Axis systems.

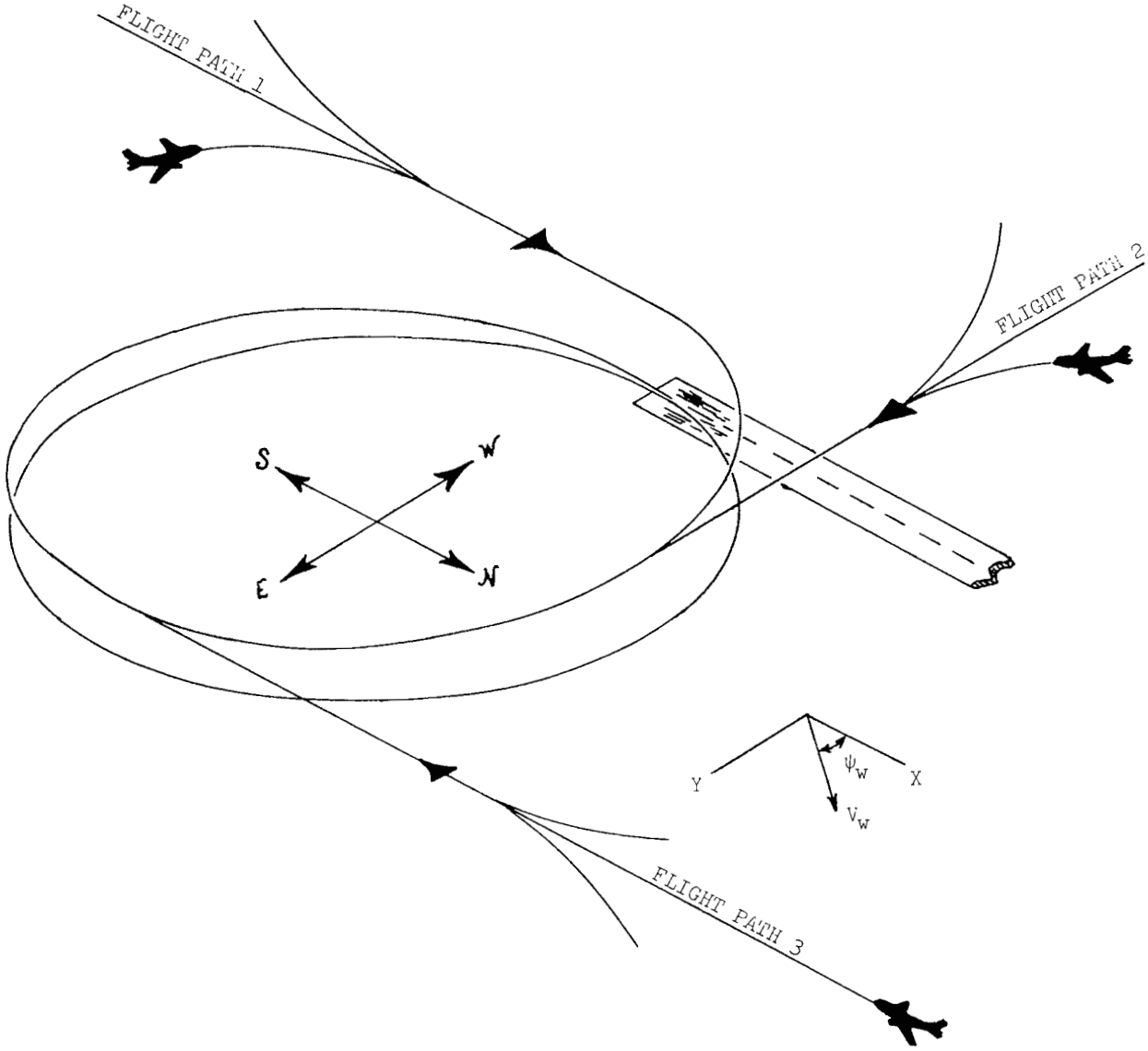

Figure 3.- Nominal flight paths.

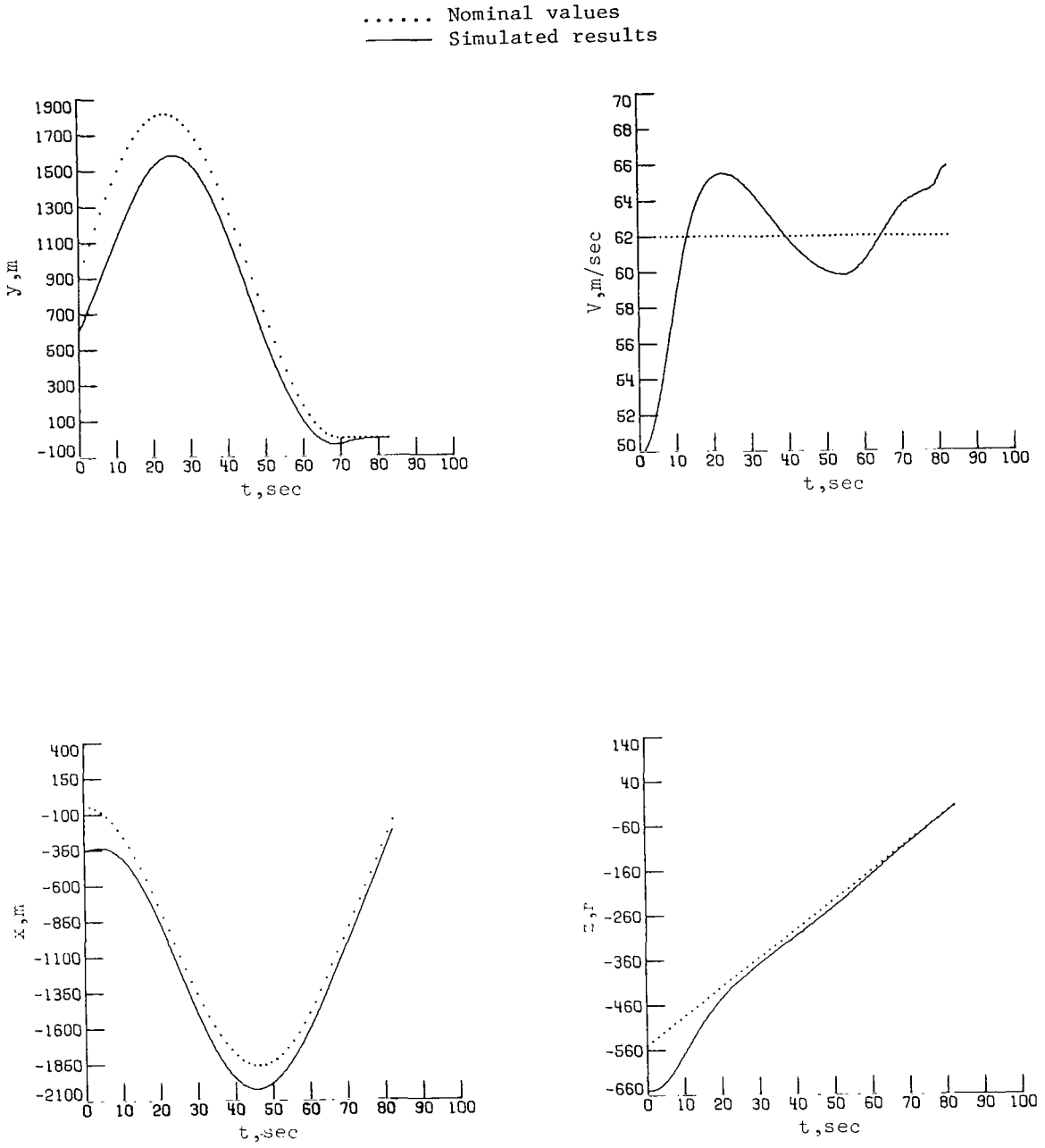

Figure 4.- State and control time histories from a representative flight. Flight path 2A; descent angle 6°; large initial errors; 15 knot east wind.

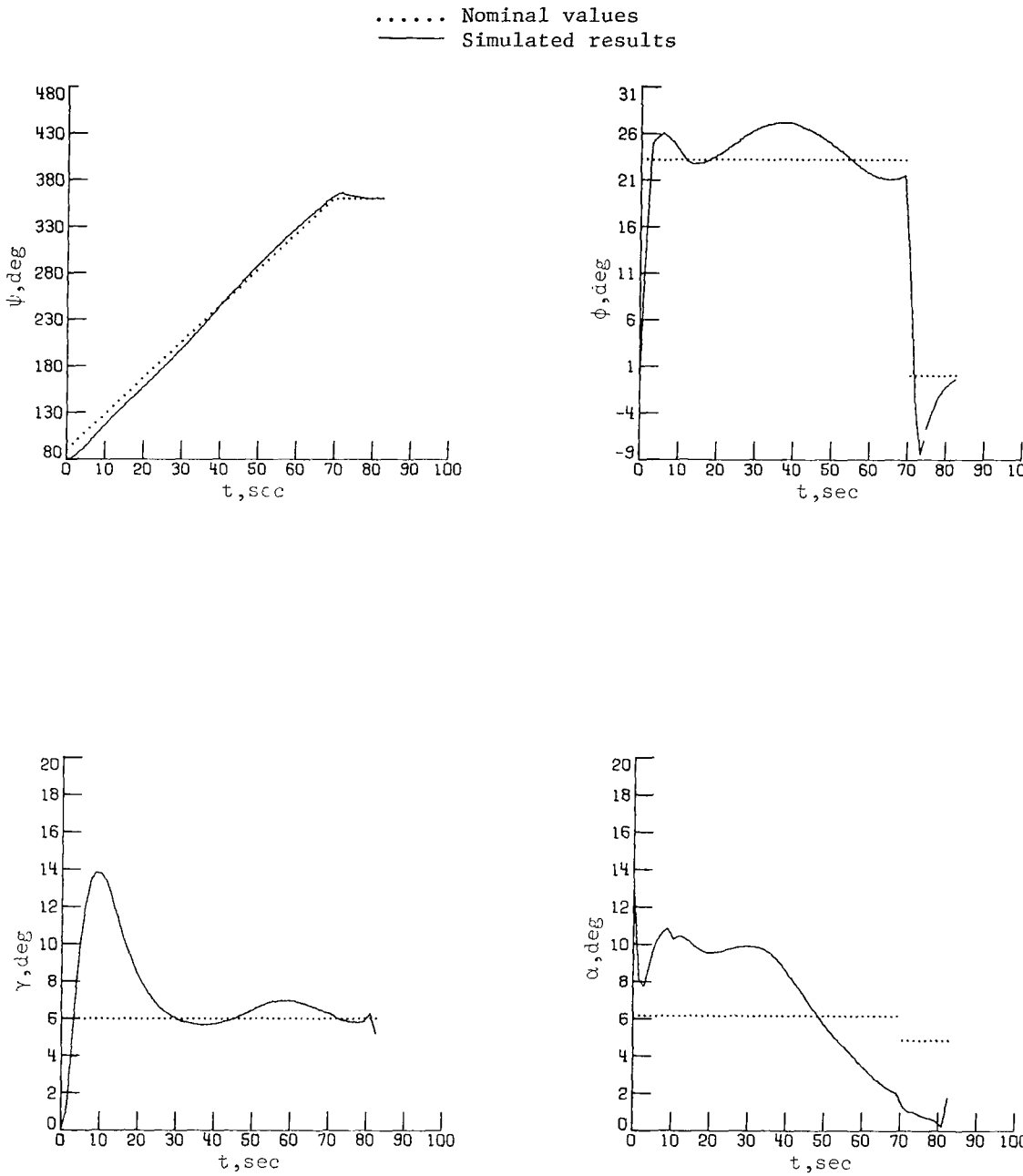

Figure 4.- Continued.

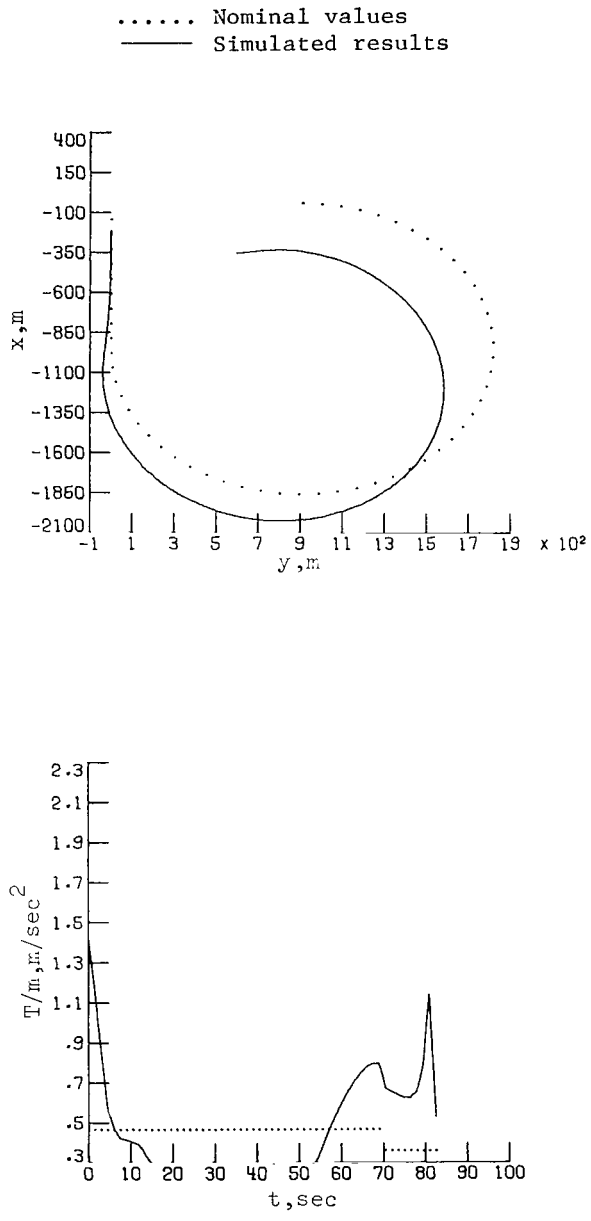

Figure 4.- Concluded.

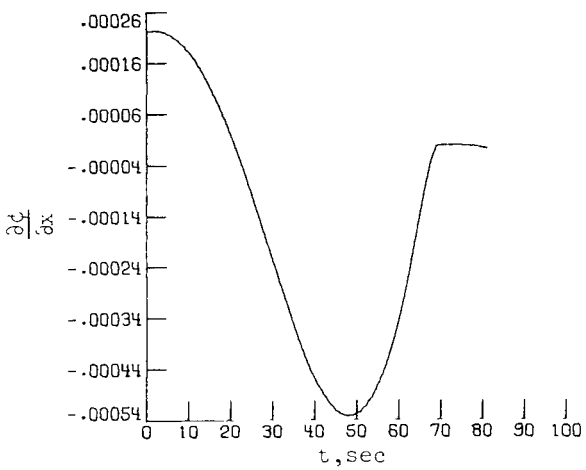

(a) K_{21}, $\partial\phi/\partial x$, 1/m.

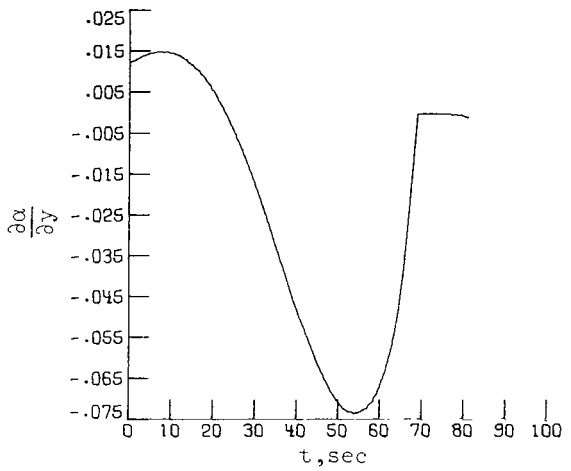

(b) K_{12}, $\partial\alpha/\partial y$, deg/m.

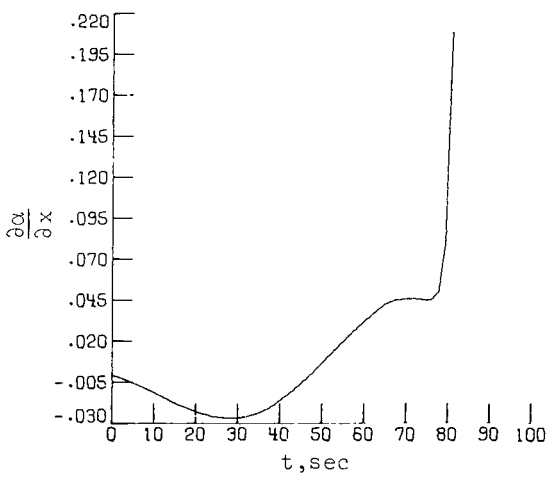

(c) K_{11}, $\partial\alpha/\partial x$, deg/m.

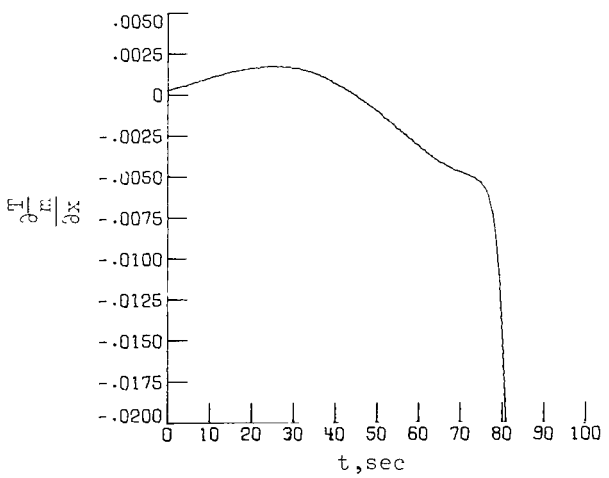

(d) K_{31}, $\frac{\partial(T/m)}{\partial x}$, $1/sec^2$.

Figure 5.- Feedback gains for flight path 2A. $\gamma = 6^o$; $\psi_0 = 90^o$; $h_0 = 550$ m.

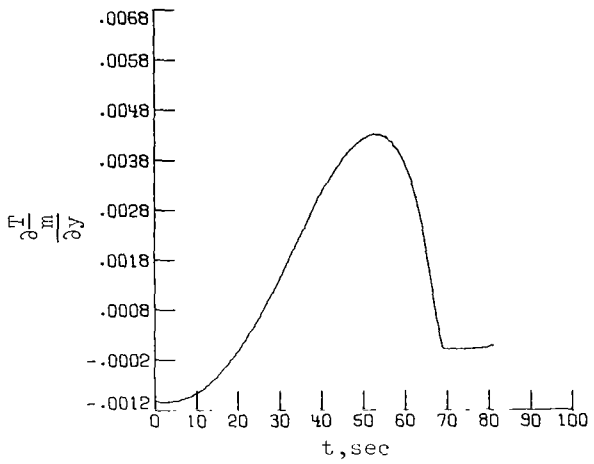

(e) K_{32}, $\frac{\partial(T/m)}{\partial y}$, $1/sec^2$.

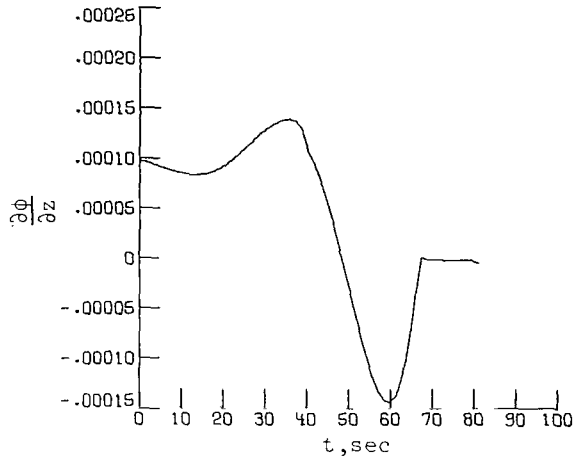

(f) K_{23}, $\partial\phi/\partial z$, 1/m.

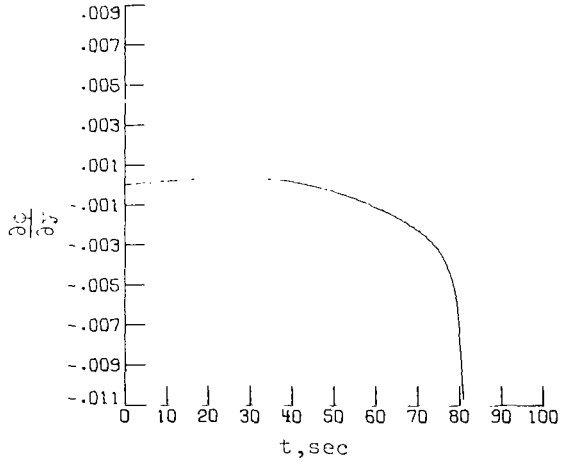

(g) K_{22}, $\partial\phi/\partial y$, 1/m.

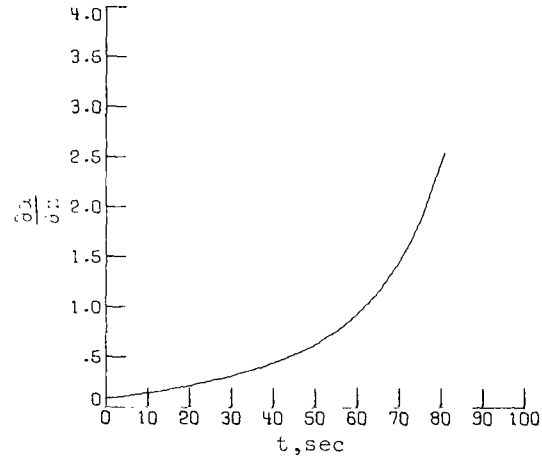

(h) K_{13}, $\partial\alpha/\partial z$, deg/m.

Figure 5.- Continued.

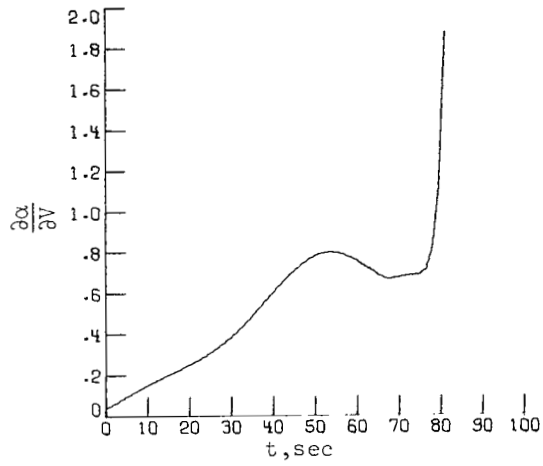

(i) K_{14}, $\partial\alpha/\partial V$, deg-sec/m.

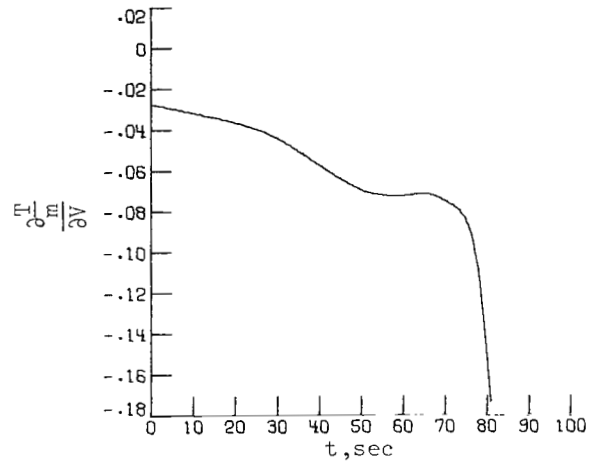

(j) K_{34}, $\frac{\partial(T/m)}{\partial V}$, 1/sec.

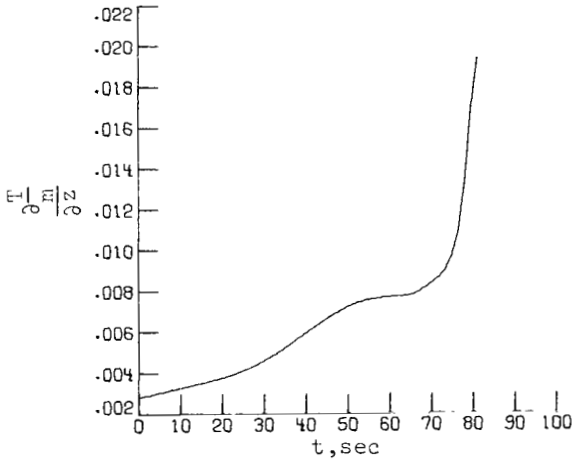

(k) K_{33}, $\frac{\partial(T/m)}{\partial z}$, $1/sec^2$.

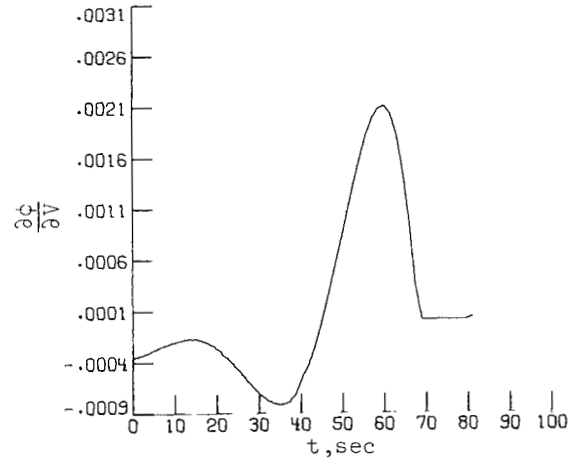

(l) K_{24}, $\partial\phi/\partial V$, sec/m.

Figure 5.- Continued.

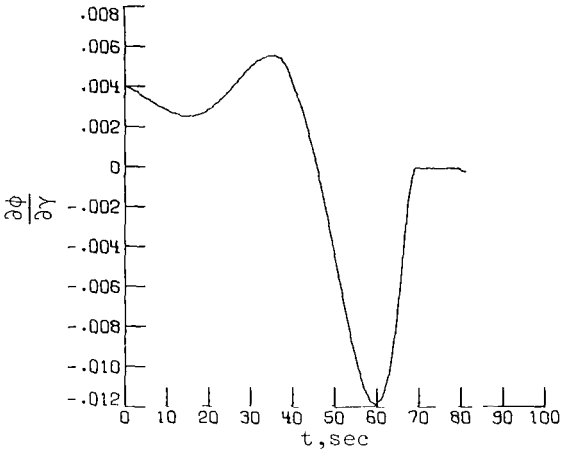

(m) K_{25}, $\partial\phi/\partial\gamma$, deg.

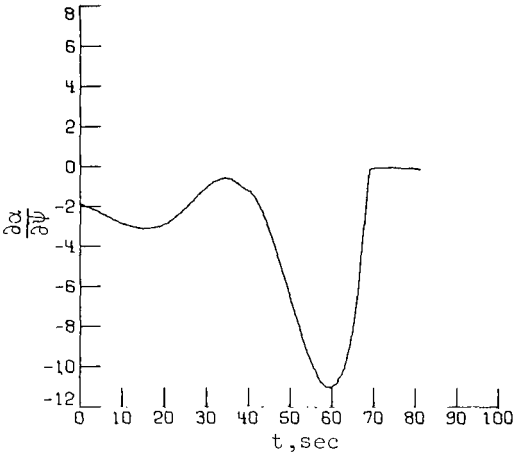

(n) K_{16}, $\partial\alpha/\partial\psi$, deg.

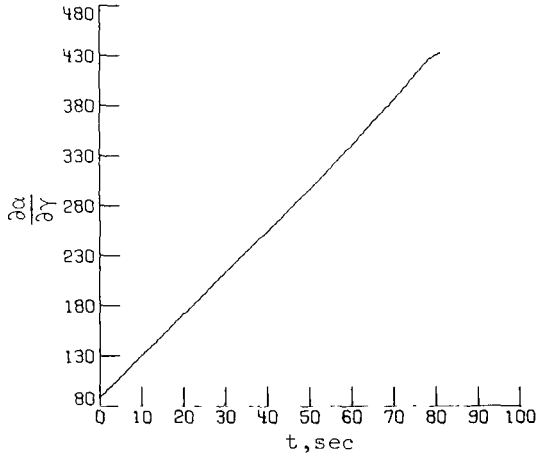

(o) K_{15}, $\partial\alpha/\partial\gamma$, deg.

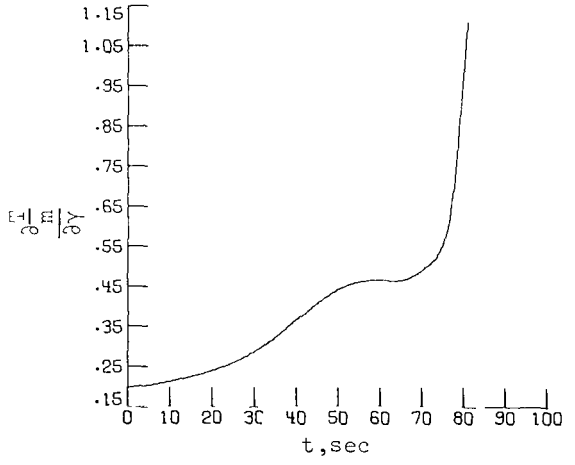

(p) K_{35}, $\frac{\partial(T/m)}{\partial\gamma}$, m/sec^2.

Figure 5.- Continued.

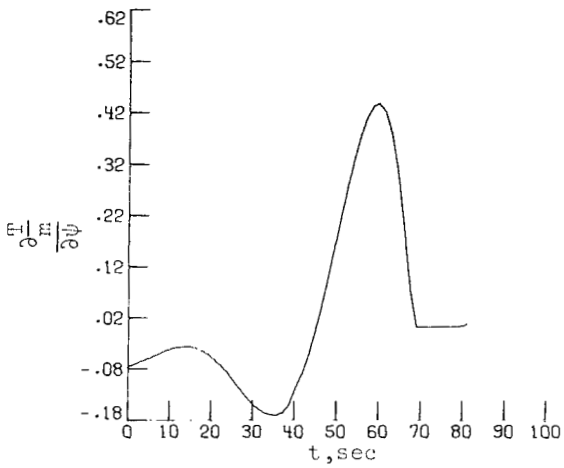

(q) K_{36}, $\frac{\partial(T/m)}{\partial\psi}$, m/sec^2.

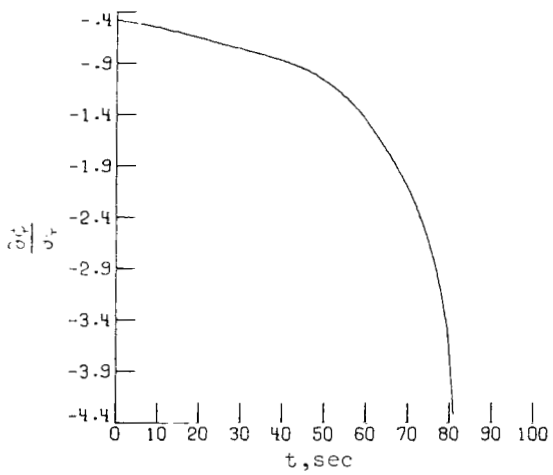

(r) K_{26}, $\partial\phi/\partial\psi$.

Figure 5.- Concluded.

NASA-Langley, 1975 L-10101

"The aeronautical and space activities of the United States shall be conducted so as to contribute . . . to the expansion of human knowledge of phenomena in the atmosphere and space. The Administration shall provide for the widest practicable and appropriate dissemination of information concerning its activities and the results thereof."

—NATIONAL AERONAUTICS AND SPACE ACT OF 1958

NASA SCIENTIFIC AND TECHNICAL PUBLICATIONS

TECHNICAL REPORTS: Scientific and technical information considered important, complete, and a lasting contribution to existing knowledge.

TECHNICAL NOTES: Information less broad in scope but nevertheless of importance as a contribution to existing knowledge.

TECHNICAL MEMORANDUMS: Information receiving limited distribution because of preliminary data, security classification, or other reasons. Also includes conference proceedings with either limited or unlimited distribution.

CONTRACTOR REPORTS: Scientific and technical information generated under a NASA contract or grant and considered an important contribution to existing knowledge.

TECHNICAL TRANSLATIONS: Information published in a foreign language considered to merit NASA distribution in English.

SPECIAL PUBLICATIONS: Information derived from or of value to NASA activities. Publications include final reports of major projects, monographs, data compilations, handbooks, sourcebooks, and special bibliographies.

TECHNOLOGY UTILIZATION PUBLICATIONS: Information on technology used by NASA that may be of particular interest in commercial and other non-aerospace applications. Publications include Tech Briefs, Technology Utilization Reports and Technology Surveys.

Details on the availability of these publications may be obtained from:

SCIENTIFIC AND TECHNICAL INFORMATION OFFICE

NATIONAL AERONAUTICS AND SPACE ADMINISTRATION

Washington, D.C. 20546